

**GLUON AND FERMION
DAMPING IN HOT QCD**

BY

KIN WAH MAK

A Thesis

Submitted to the Faculty of Graduate Studies
in Partial Fulfillment of the Requirements
for the Degree of

Doctor of Philosophy

Department of Physics
University of Manitoba
Winnipeg, Manitoba

© July, 1993



National Library
of Canada

Bibliothèque nationale
du Canada

Acquisitions and
Bibliographic Services Branch

Direction des acquisitions et
des services bibliographiques

395 Wellington Street
Ottawa, Ontario
K1A 0N4

395, rue Wellington
Ottawa (Ontario)
K1A 0N4

Your file *Votre référence*

Our file *Notre référence*

The author has granted an irrevocable non-exclusive licence allowing the National Library of Canada to reproduce, loan, distribute or sell copies of his/her thesis by any means and in any form or format, making this thesis available to interested persons.

L'auteur a accordé une licence irrévocable et non exclusive permettant à la Bibliothèque nationale du Canada de reproduire, prêter, distribuer ou vendre des copies de sa thèse de quelque manière et sous quelque forme que ce soit pour mettre des exemplaires de cette thèse à la disposition des personnes intéressées.

The author retains ownership of the copyright in his/her thesis. Neither the thesis nor substantial extracts from it may be printed or otherwise reproduced without his/her permission.

L'auteur conserve la propriété du droit d'auteur qui protège sa thèse. Ni la thèse ni des extraits substantiels de celle-ci ne doivent être imprimés ou autrement reproduits sans son autorisation.

ISBN 0-315-85982-2

Canada

Name _____

Dissertation Abstracts International is arranged by broad, general subject categories. Please select the one subject which most nearly describes the content of your dissertation. Enter the corresponding four-digit code in the spaces provided.

Elementary Particles and High Energy
 SUBJECT TERM

0798
 SUBJECT CODE

U·M·I

Subject Categories

THE HUMANITIES AND SOCIAL SCIENCES

COMMUNICATIONS AND THE ARTS

Architecture 0729
 Art History 0377
 Cinema 0900
 Dance 0378
 Fine Arts 0357
 Information Science 0723
 Journalism 0391
 Library Science 0399
 Mass Communications 0708
 Music 0413
 Speech Communication 0459
 Theater 0465

EDUCATION

General 0515
 Administration 0514
 Adult and Continuing 0516
 Agricultural 0517
 Art 0273
 Bilingual and Multicultural 0282
 Business 0688
 Community College 0275
 Curriculum and Instruction 0727
 Early Childhood 0518
 Elementary 0524
 Finance 0277
 Guidance and Counseling 0519
 Health 0680
 Higher 0745
 History of 0520
 Home Economics 0278
 Industrial 0521
 Language and Literature 0279
 Mathematics 0280
 Music 0522
 Philosophy of 0998
 Physical 0523

Psychology 0525
 Reading 0535
 Religious 0527
 Sciences 0714
 Secondary 0533
 Social Sciences 0534
 Sociology of 0340
 Special 0529
 Teacher Training 0530
 Technology 0710
 Tests and Measurements 0288
 Vocational 0747

LANGUAGE, LITERATURE AND LINGUISTICS

Language
 General 0679
 Ancient 0289
 Linguistics 0290
 Modern 0291
 Literature
 General 0401
 Classical 0294
 Comparative 0295
 Medieval 0297
 Modern 0298
 African 0316
 American 0591
 Asian 0305
 Canadian (English) 0352
 Canadian (French) 0355
 English 0593
 Germanic 0311
 Latin American 0312
 Middle Eastern 0315
 Romance 0313
 Slavic and East European 0314

PHILOSOPHY, RELIGION AND THEOLOGY

Philosophy 0422
 Religion
 General 0318
 Biblical Studies 0321
 Clergy 0319
 History of 0320
 Philosophy of 0322
 Theology 0469

SOCIAL SCIENCES

American Studies 0323
 Anthropology
 Archaeology 0324
 Cultural 0326
 Physical 0327
 Business Administration
 General 0310
 Accounting 0272
 Banking 0770
 Management 0454
 Marketing 0338
 Canadian Studies 0385
 Economics
 General 0501
 Agricultural 0503
 Commerce-Business 0505
 Finance 0508
 History 0509
 Labor 0510
 Theory 0511
 Folklore 0358
 Geography 0366
 Gerontology 0351
 History
 General 0578

Ancient 0579
 Medieval 0581
 Modern 0582
 Black 0328
 African 0331
 Asia, Australia and Oceania 0332
 Canadian 0334
 European 0335
 Latin American 0336
 Middle Eastern 0333
 United States 0337
 History of Science 0585
 Law 0398
 Political Science
 General 0615
 International Law and Relations 0616
 Public Administration 0617
 Recreation 0814
 Social Work 0452
 Sociology
 General 0626
 Criminology and Penology 0627
 Demography 0938
 Ethnic and Racial Studies 0631
 Individual and Family Studies 0628
 Industrial and Labor Relations 0629
 Public and Social Welfare 0630
 Social Structure and Development 0700
 Theory and Methods 0344
 Transportation 0709
 Urban and Regional Planning 0999
 Women's Studies 0453

THE SCIENCES AND ENGINEERING

BIOLOGICAL SCIENCES

Agriculture
 General 0473
 Agronomy 0285
 Animal Culture and Nutrition 0475
 Animal Pathology 0476
 Food Science and Technology 0359
 Forestry and Wildlife 0478
 Plant Culture 0479
 Plant Pathology 0480
 Plant Physiology 0817
 Range Management 0777
 Wood Technology 0746
 Biology
 General 0306
 Anatomy 0287
 Biostatistics 0308
 Botany 0309
 Cell 0379
 Ecology 0329
 Entomology 0353
 Genetics 0369
 Limnology 0793
 Microbiology 0410
 Molecular 0307
 Neuroscience 0317
 Oceanography 0416
 Physiology 0433
 Radiation 0821
 Veterinary Science 0778
 Zoology 0472
 Biophysics
 General 0786
 Medical 0760
EARTH SCIENCES
 Biogeochemistry 0425
 Geochemistry 0996

Geodesy 0370
 Geology 0372
 Geophysics 0373
 Hydrology 0388
 Mineralogy 0411
 Paleobotany 0345
 Paleocology 0426
 Paleontology 0418
 Paleozoology 0985
 Palynology 0427
 Physical Geography 0368
 Physical Oceanography 0415

HEALTH AND ENVIRONMENTAL SCIENCES

Environmental Sciences 0768
 Health Sciences
 General 0566
 Audiology 0300
 Chemotherapy 0992
 Dentistry 0567
 Education 0350
 Hospital Management 0769
 Human Development 0758
 Immunology 0982
 Medicine and Surgery 0564
 Mental Health 0347
 Nursing 0569
 Nutrition 0570
 Obstetrics and Gynecology 0380
 Occupational Health and Therapy 0354
 Ophthalmology 0381
 Pathology 0571
 Pharmacology 0419
 Pharmacy 0572
 Physical Therapy 0382
 Public Health 0573
 Radiology 0574
 Recreation 0575

Speech Pathology 0460
 Toxicology 0383
 Home Economics 0386

PHYSICAL SCIENCES

Pure Sciences
 Chemistry
 General 0485
 Agricultural 0749
 Analytical 0486
 Biochemistry 0487
 Inorganic 0488
 Nuclear 0738
 Organic 0490
 Pharmaceutical 0491
 Physical 0494
 Polymer 0495
 Radiation 0754
 Mathematics 0405
 Physics
 General 0605
 Acoustics 0986
 Astronomy and Astrophysics 0606
 Atmospheric Science 0608
 Atomic 0748
 Electronics and Electricity 0607
 Elementary Particles and High Energy 0798
 Fluid and Plasma 0759
 Molecular 0609
 Nuclear 0610
 Optics 0752
 Radiation 0756
 Solid State 0611
 Statistics 0463
Applied Sciences
 Applied Mechanics 0346
 Computer Science 0984

Engineering
 General 0537
 Aerospace 0538
 Agricultural 0539
 Automotive 0540
 Biomedical 0541
 Chemical 0542
 Civil 0543
 Electronics and Electrical 0544
 Heat and Thermodynamics 0348
 Hydraulic 0545
 Industrial 0546
 Marine 0547
 Materials Science 0794
 Mechanical 0548
 Metallurgy 0743
 Mining 0551
 Nuclear 0552
 Packaging 0549
 Petroleum 0765
 Sanitary and Municipal 0554
 System Science 0790
 Geotechnology 0428
 Operations Research 0796
 Plastics Technology 0795
 Textile Technology 0994

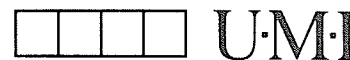
PSYCHOLOGY

General 0621
 Behavioral 0384
 Clinical 0622
 Developmental 0620
 Experimental 0623
 Industrial 0624
 Personality 0625
 Physiological 0989
 Psychobiology 0349
 Psychometrics 0632
 Social 0451



Nom _____

Dissertation Abstracts International est organisé en catégories de sujets. Veuillez s.v.p. choisir le sujet qui décrit le mieux votre thèse et inscrivez le code numérique approprié dans l'espace réservé ci-dessous.



SUJET

CODE DE SUJET

Catégories par sujets

HUMANITÉS ET SCIENCES SOCIALES

COMMUNICATIONS ET LES ARTS

Architecture 0729
 Beaux-arts 0357
 Bibliothéconomie 0399
 Cinéma 0900
 Communication verbale 0459
 Communications 0708
 Danse 0378
 Histoire de l'art 0377
 Journalisme 0391
 Musique 0413
 Sciences de l'information 0723
 Théâtre 0465

ÉDUCATION

Généralités 515
 Administration 0514
 Art 0273
 Collèges communautaires 0275
 Commerce 0688
 Économie domestique 0278
 Éducation permanente 0516
 Éducation préscolaire 0518
 Éducation sanitaire 0680
 Enseignement agricole 0517
 Enseignement bilingue et multiculturel 0282
 Enseignement industriel 0521
 Enseignement primaire 0524
 Enseignement professionnel 0747
 Enseignement religieux 0527
 Enseignement secondaire 0533
 Enseignement spécial 0529
 Enseignement supérieur 0745
 Évaluation 0288
 Finances 0277
 Formation des enseignants 0530
 Histoire de l'éducation 0520
 Langues et littérature 0279

Lecture 0535
 Mathématiques 0280
 Musique 0522
 Orientation et consultation 0519
 Philosophie de l'éducation 0998
 Physique 0523
 Programmes d'études et enseignement 0727
 Psychologie 0525
 Sciences 0714
 Sciences sociales 0534
 Sociologie de l'éducation 0340
 Technologie 0710

LANGUE, LITTÉRATURE ET LINGUISTIQUE

Langues
 Généralités 0679
 Anciennes 0289
 Linguistique 0290
 Modernes 0291

Littérature
 Généralités 0401
 Anciennes 0294
 Comparée 0295
 Médiévale 0297
 Moderne 0298
 Africaine 0316
 Américaine 0591
 Anglaise 0593
 Asiatique 0305
 Canadienne (Anglaise) 0352
 Canadienne (Française) 0355
 Germanique 0311
 Latino-américaine 0312
 Moyen-orientale 0315
 Romane 0313
 Slave et est-européenne 0314

PHILOSOPHIE, RELIGION ET THÉOLOGIE

Philosophie 0422
 Religion
 Généralités 0318
 Clergé 0319
 Études bibliques 0321
 Histoire des religions 0320
 Philosophie de la religion 0322
 Théologie 0469

SCIENCES SOCIALES

Anthropologie
 Archéologie 0324
 Culturelle 0326
 Physique 0327
 Droit 0398
 Économie
 Généralités 0501
 Commerce-Affaires 0505
 Économie agricole 0503
 Économie du travail 0510
 Finances 0508
 Histoire 0509
 Théorie 0511
 Études américaines 0323
 Études canadiennes 0385
 Études féministes 0453
 Folklore 0358
 Géographie 0366
 Gérontologie 0351
 Gestion des affaires
 Généralités 0310
 Administration 0454
 Banques 0770
 Comptabilité 0272
 Marketing 0338
 Histoire
 Histoire générale 0578

Ancienne 0579
 Médiévale 0581
 Moderne 0582
 Histoire des noirs 0328
 Africaine 0331
 Canadienne 0334
 États-Unis 0337
 Européenne 0335
 Moyen-orientale 0333
 Latino-américaine 0336
 Asie, Australie et Océanie 0332
 Histoire des sciences 0585
 Loisirs 0814
 Planification urbaine et régionale 0999
 Science politique
 Généralités 0615
 Administration publique 0617
 Droit et relations internationales 0616
 Sociologie
 Généralités 0626
 Aide et bien-être social 0630
 Criminologie et établissements pénitentiaires 0627
 Démographie 0938
 Études de l'individu et de la famille 0628
 Études des relations interethniques et des relations raciales 0631
 Structure et développement social 0700
 Théorie et méthodes 0344
 Travail et relations industrielles 0629
 Transports 0709
 Travail social 0452

SCIENCES ET INGÉNIERIE

SCIENCES BIOLOGIQUES

Agriculture
 Généralités 0473
 Agronomie 0285
 Alimentation et technologie alimentaire 0359
 Culture 0479
 Élevage et alimentation 0475
 Exploitation des pâturages 0777
 Pathologie animale 0476
 Pathologie végétale 0480
 Physiologie végétale 0817
 Sylviculture et faune 0478
 Technologie du bois 0746

Biologie
 Généralités 0306
 Anatomie 0287
 Biologie (Statistiques) 0308
 Biologie moléculaire 0307
 Botanique 0309
 Cellule 0379
 Ecologie 0329
 Entomologie 0353
 Génétique 0369
 Limnologie 0793
 Microbiologie 0410
 Neurologie 0317
 Océanographie 0416
 Physiologie 0433
 Radiation 0821
 Science vétérinaire 0778
 Zoologie 0472

Biophysique
 Généralités 0786
 Médicale 0760

Géologie 0372
 Géophysique 0373
 Hydrologie 0388
 Minéralogie 0411
 Océanographie physique 0415
 Paléobotanique 0345
 Paléoécologie 0426
 Paléontologie 0418
 Paléozoologie 0985
 Palynologie 0427

SCIENCES DE LA SANTÉ ET DE L'ENVIRONNEMENT

Économie domestique 0386
 Sciences de l'environnement 0768
 Sciences de la santé
 Généralités 0566
 Administration des hôpitaux 0769
 Alimentation et nutrition 0570
 Audiologie 0300
 Chimiothérapie 0992
 Dentisterie 0567
 Développement humain 0758
 Enseignement 0350
 Immunologie 0982
 Loisirs 0575
 Médecine du travail et thérapie 0354
 Médecine et chirurgie 0564
 Obstétrique et gynécologie 0380
 Ophtalmologie 0381
 Orthophonie 0460
 Pathologie 0571
 Pharmacie 0572
 Pharmacologie 0419
 Physiothérapie 0382
 Radiologie 0574
 Santé mentale 0347
 Santé publique 0573
 Soins infirmiers 0569
 Toxicologie 0383

SCIENCES PHYSIQUES

Sciences Pures
 Chimie
 Généralités 0485
 Biochimie 487
 Chimie agricole 0749
 Chimie analytique 0486
 Chimie minérale 0488
 Chimie nucléaire 0738
 Chimie organique 0490
 Chimie pharmaceutique 0491
 Physique 0494
 Polymères 0495
 Radiation 0754
 Mathématiques 0405

Physique
 Généralités 0605
 Acoustique 0986
 Astronomie et astrophysique 0606
 Électronique et électricité 0607
 Fluides et plasma 0759
 Météorologie 0608
 Optique 0752
 Particules (Physique nucléaire) 0798
 Physique atomique 0748
 Physique de l'état solide 0611
 Physique moléculaire 0609
 Physique nucléaire 0610
 Radiation 0756
 Statistiques 0463

Sciences Appliqués Et Technologie
 Informatique 0984
 Ingénierie
 Généralités 0537
 Agricole 0539
 Automobile 0540

Biomédicale 0541
 Chaleur et thermodynamique 0348
 Conditionnement (Emballage) 0549
 Génie aérospatial 0538
 Génie chimique 0542
 Génie civil 0543
 Génie électronique et électrique 0544
 Génie industriel 0546
 Génie mécanique 0548
 Génie nucléaire 0552
 Ingénierie des systèmes 0790
 Mécanique navale 0547
 Métallurgie 0743
 Science des matériaux 0794
 Technique du pétrole 0765
 Technique minière 0551
 Techniques sanitaires et municipales 0554
 Technologie hydraulique 0545
 Mécanique appliquée 0346
 Géotechnologie 0428
 Matières plastiques (Technologie) 0795
 Recherche opérationnelle 0796
 Textiles et tissus (Technologie) 0794

PSYCHOLOGIE

Généralités 0621
 Personnalité 0625
 Psychobiologie 0349
 Psychologie clinique 0622
 Psychologie du comportement 0384
 Psychologie du développement 0620
 Psychologie expérimentale 0623
 Psychologie industrielle 0624
 Psychologie physiologique 0989
 Psychologie sociale 0451
 Psychométrie 0632



GLUON AND FERMION DAMPING IN HOT QCD

BY

KIN WAH MAK

A Thesis submitted to the Faculty of Graduate Studies of the University of Manitoba in partial fulfillment of the requirements for the degree of

DOCTOR OF PHILOSOPHY

© 1993

Permission has been granted to the LIBRARY OF THE UNIVERSITY OF MANITOBA to lend or sell copies of this thesis, to the NATIONAL LIBRARY OF CANADA to microfilm this thesis and to lend or sell copies of the film, and UNIVERSITY MICROFILMS to publish an abstract of this thesis.

The author reserves other publications rights, and neither the thesis nor extensive extracts from it may be printed or otherwise reproduced without the author's permission.

Contents

Abstract	iv
Acknowledgements	v
list of Figures	vi
1 Introduction	1
2 Finite Temperature Field Theories	6
2.1 Linear response theory	7
2.2 Generating functional	9
3 QCD at finite temperature	20
3.1 Linear Response Analysis	22
3.2 Ward Identities and Plasma Parameters	28

4	Puzzle of the hot QCD plasma damping	32
4.1	Covariant Gauges	33
4.1.1	The plasma parameters	35
4.1.2	The static limit	38
4.2	Axial gauge	39
4.2.1	The plasma parameters	43
4.2.2	The static limit	49
4.3	Conclusions	52
5	Resummation	54
5.1	Hard thermal loops and effective propagators and vertices	55
5.1.1	Gluon propagator	56
5.1.2	Quark propagator	60
5.1.3	Three-point vertex	64
5.1.4	Four-point vertex	65
5.2	Resummation	66
5.2.1	Heavy quark	67
5.2.2	Massless quark	69
5.3	Summary	75

6 Gauge Dependence Revisited	77
7 Conclusions	84
A Frequency sums	87

Abstract

The basic formal content of field theories at non-zero temperature with application towards the stability of Quark-Gluon Plasma is presented in detail. Linear response theory is used to express the positions of the physical poles in the finite temperature gluon propagator in terms of the components of the proper self-energy. The formalism is then applied to the calculation at the one loop level of the bare plasma parameters and of Landau ghosts in two classes of gauges: the covariant gauge and a one parameter family of non-covariant gauges which interpolate between the static temporal gauge and the Coulomb gauge. The requirement of gauge invariance leads to the search of self-consistent expansion scheme rather than the usual loop expansion. In particular, one of such scheme recently developed by Braaten and Pisarski, which incorporates all relevant higher loop diagrams in terms of the “hard thermal loops”, has been used to calculate the fermion damping rate to order g^2T in the long wavelength limit. Both a heavy and a massless fermion are considered. Ward identities between the effective propagators and vertices are used to formally prove the gauge fixing independence of the damping rate to this order in a wide class of gauges. Finally, the gauge fixing dependence problem of the damping rate is revisited through the consideration of the exact cancellation of the infrared divergences in the two-loop photon polarization tensor.

Acknowledgements

I would like to express my gratitude to my advisors Randy Kobes and Gabor Kustatter for sharing their invaluable knowledge and physical insight with me and for their patience and encouragement over the past several years. Many improvements in the thesis have been brought about by their comments, suggestions and corrections. Without their support the job would have taken much longer and been done rather worse, if at all. I am indebted to many people for their help and advice during my study at Winnipeg. I would also like to thank the University of Manitoba for their financial support in the form of graduate fellowship. Finally, I thank my wife, Dannie, for her patience and support.

List of Figures

2.1	Real-time contour	18
5.1	Gluon excitations at non-zero temperature	57
5.2	Fermion excitations at non-zero temperature	62
5.3	The effective vertices: (a) Γ^μ between a quark pair and a gluon, (b) $\Gamma^{\mu\nu}$ between a quark pair and two gluons.	65
5.4	Resummed fermion propagator	67
5.5	Resummed fermion propagator	69
6.1	Two loop photon polarization tensor with the self-energy correction .	80
6.2	Two loop photon polarization tensor with the vertex correction . . .	82
A.1	One loop amplitude	91

Chapter 1

Introduction

Over the last decade, a great deal of work has been devoted to the study of field theories at finite temperature and density. The reasons for the intense study of this subject are partly motivated by the hypothetical existence of the quark-gluon plasma (QGP) phase at very high temperature and/or density. This QGP phase is then connected to the description of the early stages of the evolution of the universe [1] and may also be observable in relativistic heavy-ion collisions [2].

It has been established that at very high temperature and density hadronic matter as described by Quantum Chromodynamics (QCD) undergoes a phase transition to a state composed of quarks and gluons [3, 4, 5]. Naively speaking, this hadronic phase exists if the energy density is smaller or of the order of nuclear matter density. On the other hand, if the energy density is much larger than nuclear matter density then we are in the free quark-gluon phase. In other words, if the inter-nucleon distances are of the order or larger than in cold nuclear matter we have well indi-

vidualized hadrons. If the nuclear distances are much smaller than nuclear matter distances individual hadrons lose their identity, they mix their quarks and gluons and we have the quark-gluon plasma. In the first case, the colour degrees of freedom are, at large distances, frozen and the medium is colour neutral, quarks are bounded in hadrons. In the second case the colour degrees of freedom are present and the medium is colour conducting, quarks are liberated and move freely through the matter. Although a confinement domain has not yet been unambiguously determined, it is quite evident that an absolute confinement is excluded [6, 7]. Quarks, as well as gluons, escape the confinement region at extremely high temperature and density and become quasiparticle excitations of the hot and dense plasma.

Quantitative descriptions of QGP are reliable only when the typical energy scale for such plasmas is high which is the case when the thermodynamic parameters T, μ are large enough. Due to the asymptotic freedom of QCD, the effective charge is small in this region of the parameters [3] which leads to the existence of a weakly interacting gas of gluons and quarks and, in principle, it is possible to perform step-by-step calculations within a perturbative expansion. Elementary excitation spectra have been found and are well known [8, 9]. However, it has been found that the strong infrared behaviour of gauge theories at high temperatures generally leads in perturbation theory to a number of paradoxes [10]. Much of this stems from the apparent gauge dependence found in certain calculations, and the subsequent controversy surrounding their interpretation. For example, the gluon plasma damping constant (imaginary part of the pole position of the exact gluon temperature Green's function) in the early one loop calculations was found to be positive in the timelike axial gauge and in the Coulomb gauge [11, 12, 13], while covariant and background field gauges gave negative, gauge parameter dependent results [14, 16]. A negative

damping constant would indicate instability of the QGP thermal equilibrium state around which the perturbative expansion is performed, suggesting the existence of a lower ground state than the perturbation vacuum even in high-temperature phase. Another example is that of the Landau ghost problem [11, 17, 18, 19], where a spurious pole on the real axis appears in the static transverse gluon propagator, the location of which is gauge dependent.

Although there is a general consensus that the root of these problems lies in a failure of simple perturbation theory, there is quite strong disagreement over how to proceed next. On one hand it is argued that the plasma itself is nonperturbative in nature [20, 21], so that these problems cannot be resolved using any form of perturbation theory. On the other hand it has been argued that both the Landau ghost problem [19] and that of the damping constant [22, 23] can be resolved through a more sophisticated perturbative analysis. In particular, Pisarski [22, 23] has argued that in a gauge variant object such as the propagator there is still gauge invariant information, such as the location of the poles. Further to this he suggests that the gauge dependence found, for instance, in the one loop damping constant to order g^2T results from a breakdown of the loop expansion, but that in principle it is still possible to calculate the damping constant perturbatively by incorporating all relevant higher loop effects of the same order in g^2T which describe, physically, the collisions of an incoming plasmon with particles from the heat bath (however, regarding to complex poles see [24]). In this regard the situation is crudely analogous to the Coleman-Weinberg mechanism [25] in massless scalar electrodynamics, where the physical mass ratio predicted in the model is gauge invariant only after the loop expansion is converted to a consistent perturbative expansion involving the coupling constants [26]. General formal arguments also exist to support the conclusion that

the poles in the propagator will be gauge invariant when calculated accurately [27]. For high temperature QED and QCD such an expansion in terms of the “hard thermal loops” studied by Klimov [9], Weldon [28], Braaten and Pisarski [29], Taylor and Wong [30], and Frenkel and Taylor [31] was developed, and subsequently used to calculate the lowest order damping rate for gluons [32].

In chapter two, quantum statistical mechanics will be reviewed and the generating functional for the finite temperature Green’s functions will be derived in the form of path integral. A brief introduction to the most commonly used methods in formulating perturbative finite temperature field theory will also be given. Attention will be put on the computational techniques which are going to be used in the later chapters. In chapter three a general analysis is given of the equations determining the response of the transverse and of the longitudinal modes. We find with use of a Ward identity that these equations in the long wavelength limit are those that one would expect, but which nonetheless differ in an essential way from those that are usually used for transverse self-energies. One loop calculations of the gluon damping rate to order g^2T in both covariant and non-covariant gauges will be carried out in chapter four [33]. In chapter five, the Braaten and Pisarski resummation methods will be employed to calculate the damping rate of both the massless and heavy fermion to the same order and Ward identities between the effective propagators and vertices will be used to formally prove the gauge independence of the damping rate to this order [34]. Chapter six, which is mainly technical in content, is devoted to a recent controversy concerning the proper handling of the gauge dependent terms present in the calculation in chapter 5 and a well studied example will be given to show the need of keeping an infrared cutoff even for a finite well defined quantity [35]. Technical details for calculating frequency sums in the

imaginary time formalism will be presented in the appendix.

Chapter 2

Finite Temperature Field Theories

In the present chapter we shall discuss the basic formal content of field theories at finite temperature (for detail account see [36, 37, 38]). The generating functional for finite temperature Green's functions will be obtained in a path integral form which is especially suitable for handling the unphysical degrees of freedom that arise in constrained systems such as gauge theories. One will then be able to obtain perturbative solutions of interacting field theories in terms of "Feynman rules" analogous to the zero temperature case. In order to avoid the complexities resulting from non-commuting classical fields, in our discussion we shall be content with a study of a scalar field only, with comments about fermions and gauge bosons given along the way.

In quantum statistical mechanics, the probability of observing a state of energy E

and particle number N in the grand canonical ensemble is proportional to $e^{-\beta(E-\mu N)}$, where $\beta = 1/T$ is the inverse temperature in units where the Boltzmann's constant is set equal to one. The thermal average of an operator Q may then be expressed as

$$\langle Q \rangle = \frac{\sum_n \langle n | e^{-\beta(H-\mu N)} Q | n \rangle}{\sum_n \langle n | e^{-\beta(H-\mu N)} | n \rangle} \quad (2.1)$$

where μ is the chemical potential, $|n\rangle$ denotes an orthonormal basis and H and N are the Hamiltonian and the particle number operator respectively. It is convenient to define the partition function, Z ,

$$Z = \text{Tr} e^{-\beta(H-\mu N)}. \quad (2.2)$$

In fact, all thermodynamic properties of a system at equilibrium are completely specified by Z and its derivatives. Thus, one of the immediate tasks will be to develop methods to calculate the partition function. However, in addition to equilibrium properties, properties of physical systems can also be obtained from their response to a diversity of external probes. The results of such measurements are conveniently expressed in terms of response functions or Green's functions.

2.1 Linear response theory

Suppose an interacting system described by a time-independent Hamiltonian H with eigenstates $|j\rangle$ (in the Heisenberg picture) is perturbed from equilibrium at $t = t_0$ by an external perturbation $H_{ext}(t)$. To be specific, assume that $H_{ext}(t)$ takes the following form

$$H_{ext}(t) = \int d^3x A(\mathbf{x}, t) J(\mathbf{x}, t)$$

where J is the external source coupled to the field operator A . The linear response of the ensemble average of an Heisenberg operator $O(t)$ for $t > t_0$ is given by the first order change in the thermal expectation value arising from the external perturbation,

$$\delta \langle O(t) \rangle \equiv \langle O(t) \rangle |_{J=\delta J} - \langle O(t) \rangle |_{J=0}, \quad (2.3)$$

where the Heisenberg equation of motion of $O(t)$ is given by

$$\frac{\partial}{\partial t} O(t) = i [H + H_{ext}, O(t)] \quad (2.4)$$

and the corresponding unperturbed equation of motion of $O(t)$ is given by

$$\frac{\partial}{\partial t} O(t) = i [H, O(t)]. \quad (2.5)$$

It then follows that for a system in thermal equilibrium the rate of change of the diagonal matrix elements of $O(t)$ without the perturbation is

$$\frac{\partial}{\partial t} \langle j | O(t) | j \rangle |_{J=0} = i \langle j | [E_j, O(t)] | j \rangle = 0 \quad (2.6)$$

as expected and with the perturbation the rate is solely driven by H_{ext}

$$\begin{aligned} \frac{\partial}{\partial t} \langle j | O(t) | j \rangle |_{J=\delta J} &= i \langle j | [H + H_{ext}, O(t)] | j \rangle \\ &= i \langle j | [H_{ext}(t), O(t)] | j \rangle. \end{aligned} \quad (2.7)$$

Thus, the linear response of the field operator $A(\mathbf{x}, t)$ is given by

$$\begin{aligned} \delta \langle A(\mathbf{x}, t) \rangle &= i \int_{t_0}^t dt' Tr \rho [H_{ext}(t'), A(\mathbf{x}, t)] \\ &= -i \int_{t_0}^t dt' \int d^3 x' \delta J(\mathbf{x}', t') Tr \rho [A(\mathbf{x}, t), A(\mathbf{x}', t')] \\ &= \int_{-\infty}^{\infty} dt' \int d^3 x' \delta J(\mathbf{x}', t') D^R(\mathbf{x}, t; \mathbf{x}', t') \end{aligned} \quad (2.8)$$

where the statistical operator is

$$\rho = \frac{e^{-\beta H}}{\sum_j e^{-\beta E_j}}$$

and

$$iD^R(\mathbf{x}, t; \mathbf{x}', t') = \text{Tr} \rho [A(\mathbf{x}, t), A(\mathbf{x}', t')] \theta(t - t')$$

is the retarded Green's function of $A(x)$. The limits $t_0 \rightarrow -\infty$ and $t \rightarrow \infty$ have been taken in the last line of Eq.(2.8).

The physical response of a system to an external probe is thus characterized by correlation functions of the form $\langle A(\mathbf{x}, t) A(\mathbf{x}', t') \rangle$. This motivates the definition of real-time Green's functions which are the thermal averages of time-ordered products of operators that are convenient to calculate in perturbation theory.

2.2 Generating functional

Consider a system described by the action $S[\phi] = \int \mathcal{L}$ with the Lagrangian density \mathcal{L} depending on the relativistic field variables ϕ^i and their derivatives. Here we employ the compact notation of DeWitt, the index i encompassing both discrete and continuous (spacetime) labels associated with the fields and the Planck's constant \hbar is set equal to one. The classical equations of motion can be readily obtained by the least action principle:

$$S_{,i} \equiv \frac{\delta}{\delta \phi^i} S[\phi] = 0. \quad (2.9)$$

Suppose the action can be separated into the free field action, S_0 , which is quadratic in ϕ 's, and a piece corresponding to the interactions among the fields,

$U = \int \mathcal{U}$. Quantization of the system proceeds in the usual manner by demanding that the field variables and their conjugate momenta

$$\pi_i = \frac{\partial \mathcal{L}}{\partial \dot{\phi}^i}$$

be considered as operators and satisfy the equal time commutation relations

$$[\phi^i, \pi_j] = i\delta_j^i. \quad (2.10)$$

As mentioned before, in finite temperature field theory one is interested in calculating real-time Green's function

$$G^{1\dots m} = \langle T \phi^1 \dots \phi^m \rangle \quad (2.11)$$

defined to be the ensemble average of the time ordered product of the Heisenberg field operators. The corresponding generating functional satisfying

$$G^{1\dots m} = \frac{(-i)^m}{Z[0]} Z,^{1\dots m} \Big|_{j=0} \quad (2.12)$$

is given by

$$Z[j] = Z[0] \sum_{m=0}^{\infty} \frac{(i)^m}{m!} G^{1\dots m} j_1 \dots j_m. \quad (2.13)$$

Functional derivatives with respect to external sources j_i and field operators ϕ^i are abbreviated by a comma and subsequent upper and lower indices respectively. The summation convention is extended to include integration over continuous labels as well. The generating functional can formally be written in a more compact form as the following:

$$Z[j] = Z[0] \langle T \exp [i\phi^i j_i] \rangle. \quad (2.14)$$

We continue by specializing to the case where there is no time derivative couplings, i.e. $\dot{\phi} = \pi$. By requiring the vanishing of the expectation value of $S_{,i}$, one can verify the Dyson-Schwinger equations [39] for the generating functional

$$[\hat{S}_{,i} + j_i] Z[j] = 0 \quad (2.15)$$

where the hat appearing on top of a functional of ϕ represents the same functional form of ϕ with ϕ being replaced by $-i\frac{\delta}{\delta j}$, i.e.

$$\hat{O}[\phi] \equiv O\left[-i\frac{\delta}{\delta j}\right].$$

For instance, $\hat{\phi}^i \equiv -i\frac{\delta}{\delta j_i}$. Define the free generating functional to be the functional generated by S_0 only,

$$Z_0[j] = Z[j]|_{U=0}, \quad (2.16)$$

which satisfies the Dyson-Schwinger equations analogous to Eq.(2.15). However, under our assumption, $\hat{S}_{0,i}$ could be written as $S_{0,ij}\hat{\phi}^j$. Thus, the solution to the free Dyson-Schwinger equation is trivial and is given by

$$Z_0[j] = Z_0[0] \exp\left[-\frac{i}{2}j_l(-iG_{(0)}^{lm})j_m\right]$$

where $G_{(0)}^{lm}$ is the inverse of $-iS_{0,lm}$. The inverse, however, is not unique, as the solution is subject to boundary conditions. Nevertheless, one can verify that $G_{(0)}^{lm}$ is just the free propagator as defined in Eq.(2.12) with $U = 0$, i.e.

$$G_{(0)}^{lm} = \langle T\phi^l\phi^m \rangle_0. \quad (2.17)$$

Now, we simply take the ansatz that

$$Z[j] = F[\hat{\phi}] Z_0[j].$$

After some algebra, Eq.(2.15) could then be written as

$$i\hat{F}_{,i} Z_0 [j] = \hat{U}_{,i} Z [j]$$

and the solution for F is given by $F \sim e^{-iU}$ and hence

$$Z [j] = e^{-i\hat{U}} Z_0 [j] \quad (2.18)$$

where Eq.(2.16) has been used to set the normalization factor. Once we are able to find the free generating functional, formula (2.18) serves as a convenient starting point for the construction of a perturbation theory for calculating the Green's functions by expanding the exponent in terms of powers of \hat{U} .

Instead of restricting ourselves to the free field case, in the following we will use the path integral method to obtain the representation of the full generating functional [40]. The object of the method of path integrals is to express the generating functional entirely in terms of a classical Hamiltonian without reference to operators and states in Fock space. For the sake of clarity, the continuum space-time dependence of the field operators will be written out explicitly and all other labels will be suppressed. Let $|\phi\rangle$ be the eigenstate of the Schrodinger picture field operator $\phi_{op}(\mathbf{x})$ with eigenvalue (c-number function) $\phi(\vec{x})$,

$$\phi_{op}(\mathbf{x})|\phi\rangle = \phi(\vec{x})|\phi\rangle, \quad (2.19)$$

satisfying the completeness and orthogonality conditions

$$\int d\phi |\phi\rangle\langle\phi| = 1 \quad (2.20)$$

$$\langle\phi|\phi'\rangle = \delta(\phi - \phi'). \quad (2.21)$$

The measure $d\phi$ and the delta function $\delta(\phi - \phi')$ are formally defined to be $\prod_{\mathbf{x}} d\phi(\vec{x})$ and $\prod_{\mathbf{x}} \delta[\phi(\vec{x}) - \phi'(\mathbf{x})]$ respectively. Together with Eq.(2.19), the time evolution of the field operator,

$$\phi_{op}(\mathbf{x}, t) = e^{iHt} \phi_{op}(\mathbf{x}) e^{-iHt},$$

implies

$$\phi_{op}(\mathbf{x}, t) (e^{iHt} |\phi\rangle) = \phi(\vec{x}) (e^{iHt} |\phi\rangle). \quad (2.22)$$

One can identify $|\phi; t\rangle \equiv e^{iHt} |\phi\rangle$ as the eigenstate of the Heisenberg field operator $\phi_{op}(\mathbf{x}, t)$ at time t . It is then easy to show completeness and orthogonality conditions also hold for $|\phi; t\rangle$ as well

$$\int d\phi |\phi; t\rangle \langle \phi; t| = 1 \quad (2.23)$$

$$\langle \phi; t | \phi'; t \rangle = \delta(\phi - \phi'). \quad (2.24)$$

Similarly, in the representation where the conjugate momentum field operator, $\pi_{op}(\mathbf{x})$ is diagonal, $|\pi; t\rangle = e^{iHt} |\pi\rangle$ is the eigenstate of $\pi_{op}(\mathbf{x}, t)$

$$\pi_{op}(\mathbf{x}, t) |\pi; t\rangle = \pi(\vec{x}) |\pi; t\rangle \quad (2.25)$$

which satisfies the completeness and orthogonality conditions

$$\int d\pi |\pi; t\rangle \langle \pi; t| = 1 \quad (2.26)$$

$$\langle \pi; t | \pi'; t \rangle = \delta(\pi - \pi') \quad (2.27)$$

where the measure is defined to be $\prod_{\mathbf{x}} \frac{d\pi(\vec{x})}{2\pi}$. The overlap between the field eigenstate and its conjugate momentum eigenstate which is compatible with the equal time canonical commutation relation is given by

$$\langle \phi; t | \pi; t \rangle = \exp \left[i \int d^3x \phi(\vec{x}) \pi(\vec{x}) \right]. \quad (2.28)$$

The generating functional can now be explicitly written as the sum over all possible independent configurations ϕ' at arbitrary time t' weighted by the matrix elements of $e^{-\beta H}$

$$Z[j] = \int d\phi' \langle \phi'; t' | e^{-\beta H} T \exp \left[i \int d^4x \phi_{op}(x) j(x) \right] | \phi'; t' \rangle. \quad (2.29)$$

It can be seen almost immediately that if the real scalar field operator defined in Minkowski space is replaced by a real scalar field with time coordinate being extended to take complex values as well, then the thermal factor can be absorbed into the boundary condition on the wavefunction as

$$Z[j] = \int d\phi' \langle \phi'; t' - i\beta | T_c \exp \left[i \int_C d^4x \phi_{op}(x) j(x) \right] | \phi'; t' \rangle \quad (2.30)$$

where T_c is the generalization of the usual time ordered operator to the path ordering operator along a complex contour according to its parameterization τ ; in particular, τ at $t' - i\beta$ would be larger than τ at t' . The integrand in the exponential is now generalized to be integrated from t' to $t' - i\beta$ along a contour C which is essentially unspecified except its imaginary part must be a monotonically decreasing function of τ which guarantees the existence of the correlation functions of ϕ 's [47]. The correlation functions defined in this way are no longer the real-time Green's functions but the so-called thermal Green's functions. A path integral representation of Eq.(2.30) can be obtained in the usual manner with modifications to cope with the complex nature of the time coordinate. Dividing the contour into a number of small intervals, say N equal steps, and inserting the bras and kets of ϕ 's and π 's by using the completeness conditions of Eq.(2.23) and (2.26), together with Eq.(2.28), in the limit $N \rightarrow \infty$ the generating functional, Eq.(2.30), can be rewritten in the form

$$Z[j] = \mathcal{N}' \int D\phi D\pi \exp i \int_C d^4x \left[\pi(x) \dot{\phi}(x) - \mathcal{H}(x) + \phi(x) j(x) \right] \quad (2.31)$$

where the dot denotes the directional derivative on C and the integration measure may be written formally as

$$D\phi = d\phi' d\pi' \prod_t d\phi(t) d\pi(t). \quad (2.32)$$

Since having taken the trace, the path integration is now over all fields satisfying the periodic boundary condition

$$\phi(t' - i\beta, \mathbf{x}) = \phi(t', \mathbf{x}). \quad (2.33)$$

Note that only the field integration, and not the momentum integration, is restricted to periodic orbits. Finally, if there are no time derivative couplings as we have assumed before, the Gaussian path integral over π can be performed by completing the square to yield

$$Z[j] = \mathcal{N} \int D\phi \exp i \int_C d^4x [\mathcal{L}(x) + \phi(x)j(x)]. \quad (2.34)$$

Here, \mathcal{N} is a new temperature dependent normalization constant which is usually infinite in the $N \rightarrow \infty$ limit, but irrelevant for the calculation of the Green's functions. However, it does play a role in the canonical partition function.

For fermions, physical observables always involve even powers of the Dirac field ψ . Thus the eigenstates $|\pm\psi\rangle$ of the Schrodinger picture field operator correspond to the same values of the physical observables and describe the same state. Hence, the boundary conditions in the functional integral could either be that it is periodic or antiperiodic. To obtain a prescription which is consistent with Fermi statistics when thermal averages are calculated, it turns out to be necessary to take the matrix elements of the following form

$$\sum_{\psi} \langle \psi | \cdots | -\psi \rangle.$$

Hence, instead of having the periodic boundary condition as in the scalar case, the Grassmann integration must go over configurations with anti-periodicity in the path integral formulation of fermion fields [41].

In the case of gauge theories, the only extra complication is due to the existence of unphysical degrees of freedom, namely the longitudinal and timelike “photon” and the Faddeev-Popov ghosts [42], which cannot be in equilibrium with a heat bath. However, since the ghost fields arise from a determinant defined in the space of gauge fields in the standard Faddeev-Popov method, one should treat the ghosts as having the same periodicity in τ as the unphysical gauge fields, which, for convenience can be taken to be the same as the usual scalar field [43].

The traditional choice and perhaps the most obvious choice of the contour in the path integral of the quantum statistics is the Matsubara contour [44]: a straight line running along the imaginary axis from $t = 0$ to $t = -i\beta$. Thus the parameterization τ can simply be defined as $\tau = it$ and the generating functional is given by

$$Z[j] = \mathcal{N} \int D\phi e^{-S_E[\phi]}, \quad (2.35)$$

with

$$S_E[\phi] = \int_0^\beta d\tau \int d^3x [\mathcal{L}_E - \phi(\vec{x})j(\vec{x})] \quad (2.36)$$

$$\mathcal{L}_E(\phi(\vec{x}), \vec{x}) = -\mathcal{L}(\phi(x), x) \quad (2.37)$$

where $\bar{x}_\mu = (\tau, \vec{x})$ and $\bar{\partial}_\mu = (\frac{\partial}{\partial\tau}, \nabla)$. This so-called imaginary time formalism (ITF) has the well known advantage of having the same perturbative diagrams as in the vacuum theory. The major difficulty is that one has to deal with the euclidean propagator and an analytic continuation is needed to go back to the physical region. The analytic continuation is non-trivial in more than two external momenta.

Together with the periodicity condition of Eq.(2.33), the free propagator $G_{(0)}(\vec{x}) \equiv i\Delta(\tau, \vec{x})$ defined in Eq.(2.17) is also periodic in τ , $\Delta(\tau + \beta) = \Delta(\tau)$. Its Fourier transform

$$\Delta(\omega_n, \vec{p}) = \int_0^\beta d\tau \int d^3x e^{i(\omega_n\tau + \mathbf{p}\cdot\mathbf{x})} \Delta(\tau, \vec{x}) \quad (2.38)$$

defines the Matsubara frequencies $\omega_n = 2\pi nT$ with integer n . Inverse Fourier transform allows one to write the euclidean propagator as

$$\Delta(\tau, \mathbf{x}) = T \sum_{n=-\infty}^{\infty} \int \frac{d^3p}{(2\pi)^3} e^{-i(\mathbf{p}\cdot\mathbf{x} + \omega_n\tau)} \Delta(\omega_n, \vec{p}). \quad (2.39)$$

On the other hand, the Matsubara frequencies for fermions are odd multiples of πT , $\omega_n = \pi(2n + 1)T$, due to their antiperiodic boundary conditions at finite temperature. Here we simply state the substitutions needed for going from the vacuum perturbation expansion to the case of finite temperature in the ITF:

$$\frac{1}{i} \int \frac{d^4k}{(2\pi)^4} \rightarrow T \sum_{n=-\infty}^{\infty} \int \frac{d^3k}{(2\pi)^3}, \quad (2.40)$$

$$2\pi\delta(\sum_i k_i) \rightarrow \beta 2\pi\delta(\sum_i \mathbf{k}_i)\delta_{\omega,0}, \quad \omega = \sum_i \omega_i. \quad (2.41)$$

After calculating a particular Feynman diagram using the above prescriptions, the corresponding real-time Green's function can be obtained by analytic continuation of all the discrete external energies back to the physical region. For instance, the thermal propagator will be converted to the retarded or advanced propagator if the following continuation is made:

$$i\omega_n = 2\pi n iT \rightarrow p_0 \pm i\epsilon \quad (2.42)$$

where the limit $\epsilon \rightarrow 0^+$ should be imposed at the end of the calculations.

Choices other than the Matsubara contour also exist. One of the most popular choice, the so-called "real-time" contour, is shown in Fig. 2.1 (where the limit

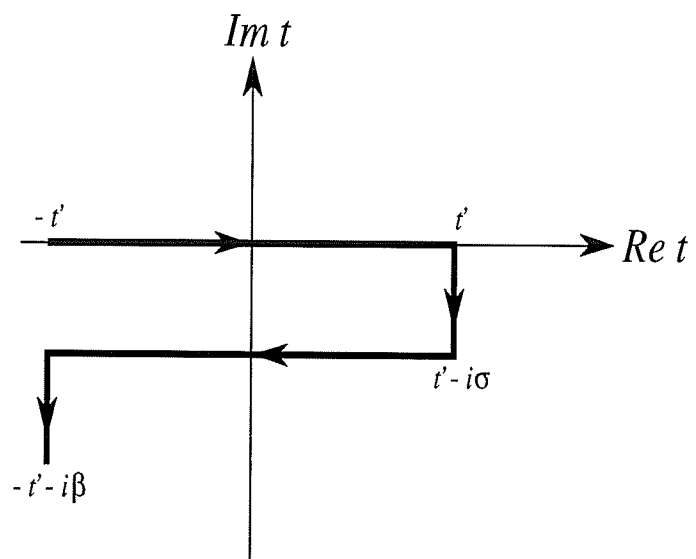


Figure 2.1: Real-time contour

$t' \rightarrow \infty$ is understood), which for obvious reasons has the advantage that no analytic continuation is required but it involves a doubling of degrees of freedom which makes calculation a bit more complicated [45]. We will use ITF in chapter 5 and real time formalism (RTF) in chapter 6. Before leaving this chapter, we simply state without proof that one may take over the renormalization prescriptions of the vacuum theory to eliminate all ultraviolet divergencies of the corresponding field theory at finite temperature and density [46].

Chapter 3

QCD at finite temperature

Quantum chromodynamics is understood as an extension of quantum electrodynamics to non-abelian gauge fields that transform according to the colour $SU(3)$ group. The general formalism of chapter 2 will now be applied to a neutral plasma (i.e. having no chemical potential) of an $SU(N)$ gauge theory coupled to N_f flavour multiplet fermions denoted collectively by $\psi(x)$. The corresponding generating functional for connected Green's functions $W[J, \xi; T, V]$ is given by

$$e^{iW[J, \xi; T, V]} = \mathcal{N} \int \mathcal{D}A_\mu \mathcal{D}\bar{\eta} \mathcal{D}\eta \mathcal{D}\bar{\psi} \mathcal{D}\psi e^{-S_E} \quad (3.1)$$

where $A_\mu^a(x)$ ($a = 1, \dots, N^2 - 1$) denote the “gluon fields”, and the Grassmann variables $\eta(x)$ and its conjugate $\bar{\eta}(x)$ are the so called Faddeev-Popov ghosts. The dependence on temperature T and volume V enters in the action $S_E(T, V)$ through the integration limits for the four-dimensional space-time integral over the QCD Lagrangian:

$$S_E = \int_0^\beta d\tau \int_V d^3x \left[\mathcal{L}_E - J^a \cdot A^a - \bar{\xi} \psi - \bar{\psi} \xi \right] \quad (3.2)$$

where $J_a^\mu(x)$ is a c-number vector source, $\xi(x)$ is an anticommuting c-number spinorial source. The corresponding Lagrangian in Minkowski space is given by

$$\mathcal{L} = \mathcal{L}_{gluon} + \mathcal{L}_M(\psi, D_\mu\psi) \quad (3.3)$$

where \mathcal{L}_{gluon} is the dynamical Lagrangian of pure gluon fields in a general gauge choice $\mathcal{F}[A_\mu] = 0$:

$$\mathcal{L}_{gluon} = -\frac{1}{4}F_{\mu\nu}^a F_a^{\mu\nu} - \frac{\lambda}{2}(\mathcal{F}^a[A_\mu])^2 + \bar{\eta}^a \mathcal{F}^a[D_\mu\eta] \quad (3.4)$$

where λ is the gauge parameter, and

$$\mathcal{L}_M = \bar{\psi}(i\gamma^\mu D_\mu - M)\psi \quad (3.5)$$

describes the gauge-invariant interaction of the fields $A_\mu(x)$ and $\psi(x)$ and is deduced from the free Lagrangian of the fields Ψ by replacing ordinary derivatives with covariant ones, $D_\mu = \partial_\mu - gA_\mu^a T^a$, such that the derivative $D_\mu\psi$ transforms covariantly with ψ under the gauge transformations

$$\psi \rightarrow U(x)\psi \quad (3.6a)$$

$$A_\mu = A_\mu^a T^a \rightarrow UA_\mu U^{-1} + \frac{i}{g}U\partial_\mu U^{-1} \quad (3.6b)$$

with $U(x) = e^{-i\omega}$, where $\omega = \omega^a T^a$ and T^a being the generators of the Lie algebra of the $SU(N)$ group. The choice of representation of the generators in different situations should be clear from the context. Here $F_{\mu\nu} = F_{\mu\nu}^a T^a = \partial_\mu A_\nu - \partial_\nu A_\mu + ig[A_\mu, A_\nu]$ denotes the gluonic field strength tensor and M is a colour-independent mass matrix in the flavour indices.

The fact that in the Hamiltonian formulation the generating functional is a trace over all possible states of the system is in the Euclidean formulation reflected in the

temporal boundary conditions for the fields. While the bosonic fields $A_\mu(\tau, \mathbf{x})$ and the ghost fields obey periodic bounding conditions in Euclidean time, $A_\mu(\beta, \mathbf{x}) = A_\mu(0, \mathbf{x})$, the fermionic fields $\bar{\psi}, \psi$ obey anti-periodic boundary conditions in this direction of space-time.

3.1 Linear Response Analysis

For QCD at finite temperature, the linear response of the gluon fields $A_\mu^a(x)$ to the external perturbation is given by

$$\delta \bar{A}_\mu^a(x) = \int dy D_{\mu\nu}^{ab}(x, y) \delta J_a^\nu(y) \quad (3.7)$$

where

$$\begin{aligned} \delta \bar{A}_\mu^a(x) &= \delta \langle A_\mu^a(x) \rangle_J \\ &= \langle A_\mu^a \rangle_J \Big|_{J=\delta J} - \langle A_\mu^a \rangle_J \Big|_{J=0} \end{aligned} \quad (3.8)$$

is the variation of the thermal average of the vector potential under the influence of a small perturbation in the external source δJ_a^ν and

$$D_{\mu\nu}^{ab}(x, y) \equiv \langle A_\mu^a(x) A_\nu^b(y) \rangle_J \Big|_{J=0} \quad (3.9)$$

is the finite temperature (retarded) gluon correlation function. We further assume that δJ_a^ν is conserved with respect to the background field, which in this case is chosen to be zero, so that

$$D_\mu^{ab} \delta J_b^\mu = \partial_\mu \delta J^{\mu a} = 0 \quad (3.10)$$

With n^μ being the velocity of the heat bath, the momentum space propagator can in general be expanded in terms of the following basis:

$$\{A_{\mu\nu}, \tilde{n}_\mu \tilde{n}_\nu, \tilde{n}_\mu k_\nu + k_\mu \tilde{n}_\nu, k_\mu k_\nu\} \quad (3.11)$$

where

$$\tilde{n}_\mu = P_{\mu\nu} n^\nu \equiv \left(g_{\mu\nu} - \frac{k_\mu k_\nu}{k^2} \right) n^\nu \quad (3.12)$$

is the transverse projection of the velocity of the heat bath with respect to the momentum k_μ , i.e. $\tilde{n}_\mu k^\mu = 0$, and

$$A_{\mu\nu} = P_{\mu\nu} - \frac{\tilde{n}_\mu \tilde{n}_\nu}{\tilde{n}^2} \quad (3.13)$$

is the projection operator satisfying $k^\mu A_{\mu\nu} = 0 = \tilde{n}^\nu P_{\mu\nu}$. Since symmetry demands that the gluon propagator be diagonal in colour space, we henceforth drop colour indices for simplicity and assume the gluon propagator takes the following form:

$$D_{\mu\nu}(k) = \frac{1}{k_t^2} A_{\mu\nu} + \frac{1}{k_l^2} \frac{\mathcal{U}_\mu \mathcal{U}_\nu}{\tilde{n}^2} + \frac{1}{\gamma} \frac{k_\mu k_\nu}{k^4} \quad (3.14)$$

where

$$\mathcal{U}_\mu = \tilde{n}_\mu + \delta(k) k_\mu \quad (3.15)$$

and at this moment k_t^2, k_l^2, δ and γ are simply treated as expansion coefficients (in fact functions of k_μ) and their physical interpretation will be given later, which will also justify the above notation.

The inverse propagator can be easily found to be

$$D_{\mu\nu}^{-1}(k) = k_t^2 A_{\mu\nu} + k_l^2 \frac{\tilde{n}_\mu \tilde{n}_\nu}{\tilde{n}^2} + \gamma \mathcal{V}_\mu \mathcal{V}_\nu \quad (3.16)$$

where

$$\mathcal{V}_\mu = k_\mu - \frac{k^2 \delta}{\tilde{n}^2} \tilde{n}_\mu \quad (3.17)$$

such that $\mathcal{U}_\mu \mathcal{V}^\mu = 0$. In the rest frame of the plasma $n^\nu = \delta^{0\nu}$,

$$A_{\mu\nu} = \begin{pmatrix} 0 & 0 \\ 0 & -\delta_{ij} + \hat{k}_i \hat{k}_j \end{pmatrix} \quad (3.18)$$

projects out the spatially transverse physical gluon mode. The presence of such a preferred frame at finite temperature accounts for the fact that the gluon propagator has in general two independent transverse components, the spatially transverse component, k_t^2 , and the spatially longitudinal component, k_l^2 . Since the decomposition in (3.14) contains only one such preferred frame, we are effectively restricting the choice of gauges to those which involve only one such four vector. Thus, at finite temperature, our analysis does not apply to light cone gauge calculations, for example.

It is believed that isotropic QCD matter in the QGP phase can support both longitudinal and transverse plasma oscillations. To extract the physical content of (3.7) it is useful to separate vectors transverse and longitudinal to the spatial vector k_i by decomposing the vectors $\delta \bar{A}_i$ and δJ^i into the following:

$$\delta \bar{A}_i^t \equiv \left(\delta_{ij} - \frac{k_i k_j}{\vec{k}^2} \right) \delta \bar{A}^j \quad (3.19a)$$

$$\delta \bar{A}_i^L \equiv \frac{k_i k_j}{\vec{k}^2} \delta \bar{A}^j \quad (3.19b)$$

$$\delta J_i^t \equiv \left(\delta_{ij} - \frac{k_i k_j}{\vec{k}^2} \right) \delta J^j. \quad (3.19c)$$

In terms of the decomposition (3.14), Eq.(3.7) can now be written as:

$$\delta \bar{A}_0 = \frac{1}{k_l^2 \tilde{n}^2} (\tilde{n}^2 - k_0 \delta) (\delta J^0), \quad (3.20a)$$

$$\delta \bar{A}_i^t = \frac{1}{k_t^2} (\delta J_i^t), \quad (3.20b)$$

$$\delta \bar{A}_i^L = \frac{k_i}{k_i^2 \tilde{n}^2} \left(\frac{k_0}{k^2} - \delta \right) (\delta J^0). \quad (3.20c)$$

Suppressing the mode of excitation, colour and spatial indices, the response of the field is given by

$$\begin{aligned} \delta \bar{A}(t) &\sim \int dk_0 e^{-ik_0 t} \delta \bar{A}(k_0) \\ &\sim \int dk_0 e^{-ik_0 t} D^R(k_0) \delta J(k_0). \end{aligned} \quad (3.21)$$

Assuming $D^R(k_0)$ has a pole at $k_0 = \omega_p(\mathbf{k}) - i\gamma(\mathbf{k})$, then carrying out the k_0 integration in Eq(3.21) leads to

$$\delta \bar{A}(t) \sim \int dt' e^{-i\omega_p(t-t')} e^{-\gamma(t-t')} \dots \quad (3.22)$$

Thus the response will oscillate with a characteristic frequency ω_p and damp in a characteristic time $1/\gamma$. Both parameters thus represent physical quantities, and therefore should be independent of any gauge fixing condition used to define the propagator.

Although Eqs.(3.20) appear to describe three independent modes it will be shown that the pole structure of the temporal and longitudinal modes is identical. Thus, as expected there are only two independent modes: the spatially transverse gluon mode and a collective longitudinal mode.

In order to analyze the pole structure of the full propagator it is useful to use Dyson's equation to express the propagator in terms of the gluon proper self-energy $\Pi^{\mu\nu}$:

$$D_{\mu\nu}^{-1} = D_{(0)}^{-1\mu\nu} + \Pi^{\mu\nu}, \quad (3.23)$$

where

$$D_{(0)}^{-1\mu\nu} = \frac{\delta^2(S_{gluon})}{\delta A_\mu \delta A_\nu} \quad (3.24)$$

is the bare inverse propagator derived from the gauge fixed classical action. Note that no approximation will be made in the following analysis; in the Conclusions we comment on the importance of calculating $\Pi_{\mu\nu}$ in a self-consistent approximation scheme.

In terms of the decomposition used above, the self-energy and the bare propagator take the form:

$$\Pi^{\mu\nu} = \Pi A^{\mu\nu} + \chi \tilde{n}^\mu \tilde{n}^\nu + \Phi(\tilde{n}^\mu k^\nu + \tilde{n}^\nu k^\mu) + \Lambda k^\mu k^\nu \quad (3.25)$$

$$D_{(0)}^{\mu\nu} = \frac{1}{k^2} A^{\mu\nu} + \frac{1}{k^2} \frac{\mathcal{I}^\mu \mathcal{I}^\nu}{\tilde{n}^2} + \frac{1}{C_{(0)}} \frac{k^\mu k^\nu}{k^4} \quad (3.26)$$

with

$$\mathcal{I}_\mu = \tilde{n}_\mu + D_{(0)} k_\mu. \quad (3.27)$$

In obtaining the bare propagator, we require that the transverse part of the bare propagator is gauge fixing independent. The gauges used in Eq.(3.26) includes as special cases the usual covariant gauges as well as classes of axial gauges [48, 33]. The inverse bare propagator can be found to be given by

$$D_{(0)}^{-1\mu\nu} = k^2 P^{\mu\nu} + C_{(0)} \mathcal{F}^\mu \mathcal{F}^\nu \quad (3.28)$$

where

$$\mathcal{F}_\mu = k_\mu - \frac{k^2 D_{(0)}}{\tilde{n}^2} \tilde{n}_\mu \quad (3.29)$$

such that $\mathcal{I}_\mu \mathcal{F}^\mu = 0$.

We can now evaluate the propagator in terms of the components of the self-energy:

$$k_t^2 = k^2 + \Pi \quad (3.30a)$$

$$\gamma = \Lambda + C_{(0)} \quad (3.30b)$$

$$\delta = \frac{1}{\Lambda + C_{(0)}} \left(C_{(0)} D_{(0)} - \frac{\tilde{n}^2}{k^2} \Phi \right) \quad (3.30c)$$

$$k_t^2 = k^2 + \chi + k^2 D_{(0)} \left[C_{(0)} - \frac{\left(C_{(0)} - \frac{\tilde{n}^2 \Phi}{k^2 D_{(0)}} \right)^2}{\Lambda + C_{(0)}} \right]. \quad (3.30d)$$

The equations for the physical modes can now be written in terms of the self-energy and bare inverse propagator:

$$\delta \bar{A}_0 = \left(1 + \frac{k_0(k^2 C_{(0)} D_{(0)} - \tilde{n}^2 \Phi)}{k^2(\Lambda + C_{(0)})} \right) \frac{1}{k_t^2} \delta J^0 \quad (3.31a)$$

$$\delta \bar{A}_i^t = \left(\frac{1}{k^2 + \Pi} \right) \delta J_i^t \quad (3.31b)$$

$$\delta \bar{A}_i^L = - \left(1 - \frac{k^2 C_{(0)} D_{(0)} - \tilde{n}^2 \Phi}{k_0(\Lambda + C_{(0)})} \right) \frac{1}{k_t^2} \frac{k_0}{k^2} k_i \delta J_0 \quad (3.31c)$$

The pole for the transverse mode is therefore given by

$$k_t^2 = k^2 + \Pi = 0 \quad (3.32)$$

which depends only on the transverse part of the self-energy. For the longitudinal modes of (3.31a) or (3.31c), the two equations will yield precisely the same poles providing the numerators have no zeroes or poles in the region of momentum space of physical interest. Note from (3.30d) that these equations appear to contain contributions from the non-transverse components of the self energy. In the next

section, we will use a Ward identity to simplify the equations and to show that in a large number of cases only the transverse components of $\Pi_{\mu\nu}$ contribute.

3.2 Ward Identities and Plasma Parameters

The Ward identity just alluded to that will be useful in analyzing the equations for the longitudinal mode can be derived from Lagrangians with a linear gauge fixing condition of the form

$$S_{g.f} = -\frac{\lambda}{2} \int dx (\mathcal{F}^\mu A_\mu)^2 \quad (3.33)$$

where \mathcal{F}^μ is independent of the quantum field A_μ . One can then show that the following identity holds [49]:

$$C_{(0)} \mathcal{F}^\mu \mathcal{F}^\nu D_{\mu\nu} = 1 \quad (3.34)$$

where $D_{\mu\nu}$ is the full propagator. Using Dyson's equation, one can then find the following relationship between the non-transverse components Φ and Λ of the self energy (2.13).

$$\Lambda (k^2 + \chi) = \tilde{n}^2 \Phi^2 \quad (3.35)$$

Substituting Eq.(3.35) into the expression for k_l^2 yields

$$k_l^2 = \frac{C_{(0)}}{(\Lambda + C_{(0)})(k^2 + \chi)} \left[k^2 + \chi + k^2 D_{(0)} \Phi \right]^2. \quad (3.36)$$

Assuming $C_{(0)}/(\Lambda + C_{(0)})$ and the numerators of the equations for longitudinal modes (3.31a) and (3.31c) to be well-behaved in the region of interest, both modes are determined by the same physical pole, namely:

$$k^2 + \chi = -k^2 D_{(0)} \Phi. \quad (3.37)$$

As expected, there is therefore only one independent longitudinal mode. Moreover, if $k^2 D_{(0)} \Phi$ is negligible in the region of momentum space of physical interest, the longitudinal mode and the transverse mode are determined solely by the transverse parts χ and Π of the self-energy respectively. This is true in both the usual covariant gauge, in which $D_{(0)}$ vanishes identically, as well as in the family of non-covariant gauges to be discussed later in certain limits of interest. The general formal proof of the on-shell transversality of the imaginary part of the gluon self-energy up to the next to the leading order in all linear gauges also exists [50].

It is important to note that the equations for the transverse and longitudinal modes are quite general, as no approximations have been made as yet. In the next chapter we will calculate the location of the physical poles at the one loop level in both covariant and non-covariant gauges. In order to facilitate these specific calculations, it is useful to express Π , χ , Φ and Λ in terms of the space time components of the self energy $\Pi_{\mu\nu}$. In particular, we will need the following identities:

$$\begin{aligned} \Pi &= \frac{1}{2} \left[P^{\mu\nu} \Pi_{\mu\nu} + \frac{k^2}{\vec{k}^2} \tilde{n}^\mu \tilde{n}^\nu \Pi_{\mu\nu} \right] \\ &= -\frac{1}{2} \left[\delta_{ij} - \frac{k_i k_j}{\vec{k}^2} \right] \Pi_{ij} \equiv -\frac{1}{2} \Pi_{ii}^t \end{aligned} \quad (3.38)$$

$$\chi = -\frac{k^2}{\vec{k}^2} \tilde{n}^\mu \tilde{n}^\nu \Pi_{\mu\nu} \quad (3.39)$$

$$\Phi = -\frac{\tilde{n}^\mu k^\nu \Pi_{\mu\nu}}{\vec{k}^2} \quad (3.40)$$

$$\Lambda = \frac{k^\mu k^\nu \Pi_{\mu\nu}}{k^4} \quad (3.41)$$

Application of these formulas to Eq.(3.32) yields the following simple expression

for the transverse mode:

$$k_0^2 = \vec{k}^2 + \frac{1}{2} \left[\Pi_{ii} - \frac{k_i k_j}{\vec{k}^2} \Pi_{ij} \right] \quad (3.42)$$

For the longitudinal mode of (3.37), one must distinguish between the cases where the right-hand-side of (3.37) vanishes or not. If it does vanish, then with use of the Ward identity (3.35) one finds the longitudinal mode is determined by

$$k_0^2 = \frac{k_i k_j \Pi^{ij}}{\vec{k}^2} + 2 \frac{\vec{k}^2}{k^2} k_0 \Phi \quad (3.43)$$

or equivalently

$$1 = \frac{\Pi_{00}}{\vec{k}^2} + 2 \frac{k_0 \Phi}{k^2} \quad (3.44)$$

If the right-hand-side of (3.37) does not vanish, then again with the help of the Ward identity one finds the longitudinal mode is found from

$$k_0^2 = \frac{k_i k_j \Pi^{ij}}{\vec{k}^2} + 2 \frac{\vec{k}^2}{k^2} k_0 \Phi - k_0^2 D_{(0)} \Phi \quad (3.45)$$

or equivalently

$$1 = \frac{\Pi_{00}}{\vec{k}^2} - D_{(0)} \Phi \quad (3.46)$$

Thus, as can be seen from (3.42) and (3.46), when $\Phi \neq 0$ the usual expressions [11, 12, 14, 15, 16] in terms of Π_{ii} and Π_{00} used for transverse self-energies,

$$k_0^2 = \vec{k}^2 + \frac{1}{2} \left[\Pi_{ii} - \frac{k_0^2}{\vec{k}^2} \Pi_{00} \right] \quad (3.47)$$

for the transverse mode, and

$$1 = \frac{\Pi_{00}}{\vec{k}^2} \quad (3.48)$$

for the longitudinal mode, must be modified (see also the discussion of the Coulomb gauge in Ref.[13]). In both classes of gauges we use we shall show what these modifications entail in the limits considered.

Before leaving this section we show how to extract the plasma parameters from equations of the general form

$$k_0^2 = f(k_0, \vec{k}) \quad (3.49)$$

which will be directly applicable to Eqs.(3.42) , (3.45) and (3.46). One assumes that there is a solution of the form $k_0 = \omega_p - i\gamma$, with $\gamma \ll \omega_p$. To leading order, the plasma frequency is then obtained by solving:

$$\omega_p^2 = \text{Ref}(\omega_p, \vec{k}) \quad (3.50)$$

and the damping constant will be given by:

$$\gamma = \frac{\text{Im}f(\omega, \vec{k})}{\omega^2 \frac{\partial}{\partial \omega} \left[\frac{\text{Ref}(\omega, \vec{k})}{\omega^2} \right]}. \quad (3.51)$$

The convention used is that if such solutions exist, then positive γ will result in exponentially damped oscillations, while negative γ will result in anti-damping.

In the next chapter we examine high temperature QCD at the one loop level in two classes of gauges in which $k^\mu \Pi_{\mu\nu} \neq 0$, for which the preceding analysis is necessary. Note that, at this level, the coefficient Λ of the self-energy vanishes by the Ward identity (3.35), implying that $k^\mu k^\nu \Pi_{\mu\nu} = 0$ to this order. We will be looking in two limits of interest: $T \gg \omega \gg |\vec{k}|$, and extracting the plasma parameters as in (3.50) and (3.51), and also the static limit $k_0 = 0$, $T \gg |\vec{k}|$, for which the well known problem of the Landau ghost appears.

Chapter 4

Puzzle of the hot QCD plasma damping

The knowledge of the positions of poles of a Green's function is useful to investigate the behaviour of excitations of the spectrum. When gauge fields are present, however, potential difficulties exist because the Green's function or the propagator depends explicitly on the gauge fixing condition used to "regulate" the functional integral. Usually this presents no additional problems in the sense that accurate calculations of physical quantities have always yield results independent of the gauge fixing condition. However, the calculation of the damping constant in a hot gluonic plasma appears to violate this principle.

It was found that the poles of the finite temperature gluon propagator and, in particular, their imaginary parts exhibit gauge dependence as soon as they are studied beyond the leading term in a high-temperature expansion. Use of the timelike

axial gauge indicates stability of the plasma to one-loop order, while covariant and background field gauges yield to the same order a result that depends on the gauge fixing parameter used.

Results from the linear response analysis done in the previous chapter will be used to calculate the plasma parameters to one-loop order in both covariant and regulated static temporal gauge, as first done in Ref. [33]. Since we are using the bare one loop polarization tensor in analyzing the equations for the physical modes, the consistency of which must then be checked, we then ascribe no direct physical importance, for instance, to the value or especially the sign of the damping constant γ found at this level.

4.1 Covariant Gauges

The covariant gauge is defined by the gauge fixing term:

$$S_{g.f} = -\frac{1}{2\xi} \int dx (\partial_\mu A^\mu)^2 \quad (4.1)$$

with associated Faddeev-Popov term:

$$S_{F.P.} = \int dx \partial_\mu \bar{\eta}^a D_{ab}^\mu \eta^b \quad (4.2)$$

where $D_\mu^{ab} = \partial_\mu \delta^{ab} + g f^{abc} A_\mu^c$ is the covariant derivative in the adjoint representation.

The coefficients appearing in the bare propagator (3.26) are thus

$$D_{(0)} = 0 \quad (4.3a)$$

$$C_{(0)} = \frac{1}{\xi} \quad (4.3b)$$

Thus, as mentioned in the previous section, since $D_{(0)} = 0$ the right-hand-side of Eq.(3.37) for the longitudinal mode vanishes, and so this equation involves only the transverse components of the self energy.

In the one-loop approximation the polarization tensor of gluons is represented by the following diagrams

$$\frac{1}{2} \text{ (gluon loop) } + \frac{1}{2} \text{ (ghost loop) } - \text{ (quark loop) }$$

where the wavy and broken lines stand for the gluon and ghost propagators respectively. For the moment, let us leave aside the contribution from the quark loop diagram. For the Feynman rules, see Ref.[49]. The summation is carried out over even frequencies including the Green's functions of the ghost particles.

The covariant gauge self-energy at finite temperature has been calculated previously [16] so here we give only the results. The formal expression for $\Pi_{\mu\nu}$ to the one-loop level is:

$$\begin{aligned} \Pi^{\mu\nu} &= g^2 N \int dp \left[-g^{\mu\nu} D_{(0)}^{\alpha}{}_{\alpha}(p) + D_{(0)}^{\mu\nu}(p) \right] \\ &- g^2 N \int dp \frac{p^\mu q^\nu}{p^2 q^2} \\ &- \frac{1}{2} g^2 N \int dp \Gamma^{\alpha\beta\mu}(p, q, k) D_{(0)\alpha\alpha'}(p) D_{(0)\beta\beta'}(q) \Gamma^{\alpha'\beta'\nu}(p, q, k) \end{aligned} \quad (4.4)$$

with bare propagator

$$D_{(0)}^{\mu\nu}(k) = \frac{1}{2} \left[-g^{\mu\nu} + (1 - \xi) \frac{k^\mu k^\nu}{2} \right] \quad (4.5)$$

and three point interaction vertex:

$$\Gamma^{\alpha\beta\mu}(p, q, k) = g^{\alpha\beta}(p - q)^\mu + g^{\beta\mu}(q - k)^\alpha + g^{\mu\alpha}(k - p)^\beta. \quad (4.6)$$

The first line of (4.4) is from the four gluon vertex while the second is from the ghost-ghost-gluon vertex and the third is from the three gluon vertex. The conventions for internal momenta are given by $p + q + k = 0$ and we have defined:

$$\int dp \equiv T \sum_n \int \frac{d^3 p}{(2\pi)^3} \quad (4.7)$$

As shown in Ref.[16], $\Pi_{\mu\nu}$ can be expressed as follows.

$$\begin{aligned} \Pi_{\mu\nu} &= g^2 N \int dp \left\{ \frac{-4p_\mu p_\nu + 2p^2 g_{\mu\nu} + k_\mu k_\nu - 2K_{\mu\nu}}{p^2 q^2} \right. \\ &+ (1 - \xi) \left[\frac{Q_{\mu\nu} - P_{\mu\nu} - 2K_{\mu\nu}}{p^4} + \frac{k^2 K_{\mu\nu} + T_{\mu\nu}(q)}{p^4 q^2} \right] \\ &\left. - (1 - \xi)^2 \frac{K_{\mu\alpha} p^\alpha K_{\nu\beta} p^\beta}{2p^4 q^4} \right\} \quad (4.8) \end{aligned}$$

where $K_{\mu\nu} = k^2 g_{\mu\nu} - k_\mu k_\nu$, etc. and $T_{\mu\nu}(p) = K_{\mu\alpha} p^\alpha p_\nu + K_{\nu\alpha} p^\alpha p_\mu$. The important aspect of this polarization tensor relevant for the present purposes is that while $k^\mu k^\nu \Pi_{\mu\nu} = 0$, as expected from (3.35) at the one loop level since $\Lambda \sim \Phi^2$, we have $k^\mu \Pi_{\mu\nu} \neq 0$, except in the Feynman gauge ($\xi = 1$). Explicitly,

$$\begin{aligned} \Phi &= -\frac{k_\mu \Pi^{\mu 0}}{\vec{k}^2} \\ &= -\frac{1}{2}(1 - \xi) \frac{k_0 k^2}{\vec{k}^2} g^2 N \int dp \frac{\vec{k} \cdot \vec{p}}{p^4 q^2} \quad (4.9) \end{aligned}$$

4.1.1 The plasma parameters

We first look at the plasma parameters in the long wavelength, high temperature limit. In this limit, the equation for the transverse mode, (3.42), can be written as:

$$k_0^2 = \frac{1}{2} \Pi_{ii}^t \Big|_{\vec{k}^2=0} \quad (4.10)$$

where Π_{ii}^t appears in (3.38). Moreover, one finds with Φ given in (4.9) that the real part of Φ vanishes at $\vec{k}^2 = 0$ in the high temperature limit, while the imaginary part is finite:

$$\text{Im}\Phi \rightarrow \frac{1}{24\pi}(1 - \xi)g^2NT \quad (4.11)$$

Thus $\vec{k}^2\Phi = 0$ when $\vec{k}^2 \rightarrow 0$ and Eq.(3.43) for the longitudinal mode reduces to the simple expression

$$k_0^2 = \left. \frac{k_i k_j \Pi^{ij}}{\vec{k}^2} \right|_{\vec{k}^2=0} \quad (4.12)$$

The equations for the two modes are actually the same in the long-wavelength limit, as shown by the following general argument [13]: since $\Pi_{ij}(k_0, |\vec{k}|)$ vanishes at $\vec{k}^2 = 0$, rotational invariance demands that we can write $\Pi_{ij}(k_0, |\vec{k}| = 0) = \Pi(k_0)\delta_{ij}$. This then leads to the relation

$$\Pi_{ii}|_{\vec{k}^2=0} = 3 \left. \frac{k_i k_j \Pi^{ij}}{\vec{k}^2} \right|_{\vec{k}^2=0} \quad (4.13)$$

which implies the equivalence of Eqs. (4.10) and (4.12). Thus, the equations for the longitudinal and transverse modes are the same in the long wavelength limit if the self-energy is transverse to the required order of approximation. Physically, the two mass shells coincide at zero momentum because, for a particle at rest, there is no way to distinguish between transverse and longitudinal polarization.

The determination of the one loop bare plasma parameters from Eqs.(4.10) and (4.12) in this gauge is straightforward [16], and so we simply quote the results for later reference. One finds for both the transverse and longitudinal modes the values

$$\omega_p^2 = \frac{1}{9}g^2NT^2 \quad (4.14)$$

$$\gamma = -\frac{g^2NT}{24\pi} \left[5 + \frac{1}{2}(1 - \xi) + \frac{1}{4}(1 - \xi)^2 + \frac{2}{2}(1 - \xi) \right]$$

$$= -\frac{g^2 NT}{24\pi} \left[5 + \frac{3}{2}(1 - \xi) + \frac{1}{4}(1 - \xi)^2 \right] \quad (4.15)$$

As in previous calculations, the one-loop result for the damping constant is gauge fixing dependent.

It is interesting to study the longitudinal plasma parameters determined by Eq.(4.12) by expressing it in terms of Π_{00} and Φ as in (3.46) with $D_{(0)} = 0$:

$$1 = \frac{\Pi_{00}}{\vec{k}^2} \Big|_{\vec{k}^2=0} + \frac{2\Phi}{k_0} \Big|_{\vec{k}^2=0} \quad (4.16)$$

and examining the difference between employing the correct equation (4.16) as opposed to just Π_{00} as in Eq.(3.48) used for transverse polarization tensors. One can show that, while the real part of Φ does not contribute to (4.16) in the high temperature limit, its imaginary part given in (4.11) does. In fact, one can trace the first three terms in the first relation in (4.15) to the imaginary part of Π_{00} , while the remaining term can be traced to the imaginary part of Φ given in (4.11). Thus, in these gauges there is a difference between using (4.12) involving $k_i k_j \Pi^{ij}$ and using (4.16) with just Π_{00} in determining γ . Similar conclusions along these lines can be also made concerning the transverse mode.

It is worth noting that the $\xi = 0$ value of the damping constant of (4.15) agrees with the calculation in Ref. [51] using the Vilkovisky-DeWitt formalism. This is a consequence of the fact that the Vilkovisky-DeWitt formalism yields a self-energy which is precisely equal to the transverse part of the Landau gauge $\xi = 0$ self-energy presented here. What is surprising here is that while the Vilkovisky-DeWitt self-energy is transverse by construction, the Landau gauge self-energy is not transverse at one loop at finite temperature. However, there exists a general proof [52], at zero temperature, which states that the Vilkovisky-DeWitt effective action should

be equal to the Landau-DeWitt gauge effective action, and therefore generate the same two point functions. The fact that this is not the case at one loop either suggests that the proof breaks down at finite temperature, or that in a consistent perturbative expansion the non-transverse part of the self-energy should vanish.

4.1.2 The static limit

In the $k_0 = 0$ static limit, one finds that the transverse pole (3.42) is found by solving

$$\vec{k}^2 = -\frac{1}{2}\Pi_{ii}\Big|_{k_0=0} \quad (4.17)$$

where we have used the fact that $k^i k^j \Pi_{ij}$ vanishes at $k_0 = 0$. For the longitudinal pole, one sees that Φ of (4.9) vanishes at $k_0 = 0$ and so from (3.46) the equation in this case only involves Π_{00} :

$$\vec{k}^2 = \Pi_{00}\Big|_{k_0=0} \quad (4.18)$$

In the high temperature, long wavelength limit, due to the Bose enhancement, only one term of the sum over frequencies, that for which $p_0 = 0$, is essential. This leads one to calculate only the three-dimensional integral for (4.8), and the required asymptotic form is easily found to be

$$\Pi_{ij} = \left(\delta_{ij} - \frac{k_i k_j}{\vec{k}^2} \right) \left(-\frac{1}{64} (9 + 2\xi + \xi^2) g^2 N |\vec{k}| T \right) \quad (4.19)$$

and hence the equation for the transverse pole becomes [17, 18]

$$\vec{k}^2 - \frac{1}{64} (9 + 2\xi + \xi^2) g^2 N |\vec{k}| T = 0 \quad (4.20)$$

while that for the longitudinal pole is

$$\vec{k}^2 + \frac{1}{3} g^2 N T^2 - \frac{1}{4} g^2 N |\vec{k}| T = 0. \quad (4.21)$$

The dominant contribution to the change of free energy of two static charges at large separation is given by

$$V(r) \propto \frac{e^{-m_{el}r}}{r} \quad (4.22)$$

where the chromo-electric mass (inverse of the electric screening length) squared is

$$m_{el}^2 = -\Pi_{00}(k_0 = 0, k \rightarrow 0) = \frac{1}{3}g^2NT^2. \quad (4.23)$$

However, in the magnetic sector, there is no magnetic mass up to order of gT to control the infrared behaviours. In fact, the presence of a pole on the real axis for the transverse mode is the well known Landau ghost problem. This fact indicates the unreliability of ordinary perturbative calculations in the infrared region of momenta and implies that simple perturbation theory is breaking down at scales $|\vec{k}| \leq g^2NT$ [17]. Moreover, in a relativistic gauge with real ξ , the singularity persists for any ξ and so it is unlikely that this difficulty can be eliminated by the choice of gauge. The singularity found is an intrinsic difficulty of perturbative QCD and is inherent in all finite temperature Green's functions. In contrast, magnetic fields in QED remain unscreened at every order [17]. We shall not comment further on this problem, but will return to it later when we consider the same limit in a class of axial gauges, particularly the dependence of the pole on the gauge parameter ξ .

4.2 Axial gauge

The use of axial gauges in these types of calculations is motivated in part by the desirable property in these gauges that only physical modes are present so that compensating ghost terms do not seem to be needed. In practice, however, major

difficulties exist with these gauges. Most notable in the temporal axial gauge $A^0 = 0$ is the presence in the propagator of an unresolved pole at $k_0 = 0$. In the past this pole has been handled, at least at the one loop level, by the principle value prescription [53]

$$\frac{1}{k_0^2} \equiv PP \left(\frac{1}{k_0^2} \right) = \frac{1}{2} \left(\frac{1}{(k_0 + i\varepsilon)^2} + \frac{1}{(k_0 - i\varepsilon)^2} \right) \quad (4.24)$$

It has recently been suggested [54, 55], however, that the consistency of this procedure may be in doubt even at the one loop level. Another potential problem with the condition $A^0 = 0$ is that it is not compatible at finite temperature with the periodic nature of the fields [56]. To avoid both of these difficulties, we shall work in a class of gauges where there is no ambiguity in the pole structure of the propagator and that, in a certain limit of a gauge parameter, corresponds to a static temporal axial gauge, $\partial_0 A^0 = 0$ in which the unresolved pole also appears.

The class of gauges we shall use was first considered by Frenkel and Taylor [57] and later developed by Burnel [58] (see also the discussion of the static limit in Ref. [13]). In these gauges the gauge fixing term is represented as

$$S_{g.f.} = -\frac{1}{2\alpha(\alpha-1)} \int dx (n \cdot \partial n \cdot A_a - \alpha \partial \cdot A_a)^2 \quad (4.25)$$

together with associated Faddeev-Popov term

$$S_{F.P.} = - \int dx \bar{\eta}^a (n \cdot \partial n \cdot D_{ab} - \alpha \partial \cdot D_{ab}) \eta^b \quad (4.26)$$

where n_μ is a constant timelike vector, which we shall take to be $n_\mu = (1, 0, 0, 0)$.

The coefficients of the inverse propagator appearing in (2.12) are then given by

$$C_{(0)} = -\frac{k_C^4}{\alpha(1-\alpha)k^4} \quad (4.27a)$$

$$D_{(0)} = \frac{k_0 k^2}{k^2 k_C^2} \quad (4.27b)$$

where $k_C^2 = (1 - \alpha)k_0^2 + \alpha k^2$ and $a^2 = \alpha/(1 - \alpha)$ which will be assumed positive in the following. Note that for this class of gauges $D_{(0)} \neq 0$, and so in principle the right-hand-side of (3.37) might contribute to the equation for the longitudinal mode.

The bare propagator in this class of gauges is

$$D_{(0)}^{\mu\nu}(k) = -\frac{1}{k^2 + i\varepsilon} \left[g^{\mu\nu} + \frac{k^\mu k^\nu - k_0 (\delta^{0\mu} k^\nu + \delta^{0\nu} k^\mu)}{(1 - \alpha)(k_0^2 + a^2 \vec{k}^2)} \right] \quad (4.28)$$

Note that setting $\alpha = 0$ in (4.28) gives the bare temporal gauge axial propagator with the unresolved pole at $k_0 = 0$, while setting $\alpha = 1$ gives the Coulomb gauge propagator. As we shall see, however, these two limits are quite subtle, and they are best taken at the end of the calculation.

The polarization tensor in this class of gauges at the one loop level is given formally by a similar expression to that for the covariant gauges (4.4):

$$\begin{aligned} \Pi^{\mu\nu} &= g^2 N \int dp \left[-g^{\mu\nu} D_{(0)}^\alpha{}_\alpha(p) + D_{(0)}^{\mu\nu}(p) \right] \\ &- g^2 N \int dp \frac{(\delta^{0\mu} p_0 - \alpha p^\mu)(\delta^{0\nu} q_0 - \alpha q^\nu)}{(1 - \alpha)(p_0^2 + a^2 \vec{p}^2)(1 - \alpha)(q_0^2 + a^2 \vec{q}^2)} \\ &- \frac{1}{2} g^2 N \int dp \Gamma^{\alpha\beta\mu}(p, q, k) D_{(0)\alpha\alpha'}(p) D_{(0)\beta\beta'}(q) \Gamma^{\alpha'\beta'\nu}(p, q, k) \end{aligned} \quad (4.29)$$

where the conventions are as in (4.6) and (4.7) and $D_{(0)}^{\mu\nu}$ appears in (4.28).

As in the covariant gauges, one has $k^\mu k^\nu \Pi_{\mu\nu} = 0$, but $k^\mu \Pi_{\mu\nu} \neq 0$. One finds rather that Φ of (3.40) can be written in the form

$$\Phi = -\frac{k^\mu \Pi_{\mu 0}}{\vec{k}^2}$$

$$= -\frac{a^2 k_0}{\vec{k}^2} \int dp \left[\frac{(\vec{k} \cdot \vec{p})^2 - \vec{k}^2 \vec{p}^2}{p^2(1-\alpha)(p_0^2 + a^2 \vec{p}^2)(q_0^2 + a^2 \vec{q}^2)} \right] \quad (4.30)$$

For future use we list here the following components of the polarization tensor (4.29).

$$\begin{aligned} \Pi_{00}(k) &= g^2 N \int dp \frac{2}{p^2} \\ &- \frac{1}{2} g^2 N \int dp \frac{2a^2}{p^2(q_0^2 + a^2 \vec{q}^2)} \left[|\vec{q} - \vec{k}|^2 - \frac{(\vec{q}^2 - \vec{k}^2)^2}{(1-\alpha)(p_0^2 + a^2 \vec{p}^2)} - \frac{p^2 \vec{p}^2}{(p_0^2 + a^2 \vec{p}^2)} \right] \\ &- \frac{1}{2} g^2 N \int dp (p_0 - q_0)^2 \left[\frac{1}{p^2 q^2} + \frac{2}{p^2(q_0^2 + a^2 \vec{q}^2)} \right. \\ &\left. - \frac{1}{(p_0^2 + a^2 \vec{p}^2)(q_0^2 + a^2 \vec{q}^2)} + \frac{1}{p^2 q^2} \frac{(\vec{p} \cdot \vec{q})^2}{(1-\alpha)(p_0^2 + a^2 \vec{p}^2)(1-\alpha)(q_0^2 + a^2 \vec{q}^2)} \right] \end{aligned} \quad (4.31)$$

$$\begin{aligned} k^i k^j \Pi_{ij}(k) &= -g^2 N \int dp \left[\frac{\vec{k}^2}{p^2} + \frac{(\vec{k} \cdot \vec{p})^2}{p^2(1-\alpha)(p_0^2 + a^2 \vec{p}^2)} + \frac{(1-a^2)\vec{k}^2}{(p_0^2 + a^2 \vec{p}^2)} \right] \\ &- g^2 N \int dp \left\{ \frac{(\vec{k} \cdot \vec{p})^2}{(p_0^2 + a^2 \vec{p}^2)} \frac{a^2}{(q_0^2 + a^2 \vec{q}^2)} \right. \\ &\left. + (q_0 - k_0)^2 \frac{a^2}{(p_0^2 + a^2 \vec{p}^2)} \left[\frac{\vec{k}^2}{q^2} - \frac{(\vec{k} \cdot \vec{q})^2}{q^2(1-\alpha)(q_0^2 + a^2 \vec{q}^2)} \right] \right\} \\ &- g^2 N \int dp \left\{ \frac{[\vec{k} \cdot (\vec{p} - \vec{q})]^2}{p^2(q_0^2 + a^2 \vec{q}^2)} + \frac{\vec{k}^2 \vec{p}^2 - (\vec{k} \cdot \vec{p})^2}{p^2 q^2} \right. \\ &\left. + \frac{2\vec{k} \cdot \vec{p} \vec{k} \cdot (\vec{p} - \vec{q}) \vec{p} \cdot (\vec{p} - \vec{q}) - \vec{p}^2 (\vec{k} \cdot \vec{p})^2 + 2\vec{p} \cdot \vec{q} (\vec{k} \cdot \vec{p})^2 - \vec{k}^2 (\vec{p} \cdot \vec{q})^2}{p^2 q^2 (1-\alpha)(p_0^2 + a^2 \vec{p}^2)} \right\} \end{aligned} \quad (4.32)$$

$$\Pi_{ii}(k) = g^2 N \int dp \left[\frac{3a^2 - 2}{(p_0^2 + a^2 \vec{p}^2)} - \frac{4}{p^2} \right] - \frac{1}{2} g^2 N \int dp \left\{ \frac{a^4 (\vec{k}^2 - 2\vec{p} \cdot \vec{q})}{(p_0^2 + a^2 \vec{p}^2)(q_0^2 + a^2 \vec{q}^2)} \right.$$

$$\begin{aligned}
& + 2(q_0 - k_0)^2 \frac{a^2}{(p_0^2 + a^2 \vec{p}^2)} \left[\frac{2}{q^2} + \frac{1}{(q_0^2 + a^2 \vec{q}^2)} \right] \Big\} \\
& - \frac{1}{2} g^2 N \int dp \left\{ \frac{1}{p^2 q^2} \left[9 \vec{k}^2 - 20(\vec{p} \cdot \vec{q}) - 7 \vec{k}^2 \frac{(\vec{p} \cdot \vec{q})^2}{\vec{p}^2 \vec{q}^2} + 12 \frac{(\vec{p} \cdot \vec{q})^3}{\vec{p}^2 \vec{q}^2} \right] \right. \\
& + \frac{2}{q^2 (p_0^2 + a^2 \vec{p}^2)} \left[\vec{k}^2 + 4 \vec{p} \cdot \vec{q} + 6 \frac{(\vec{p} \cdot \vec{q})^2}{\vec{p}^2} + \vec{k}^2 \frac{(\vec{p} \cdot \vec{q})^2}{\vec{p}^2 \vec{q}^2} \right] \\
& \left. + \frac{\vec{k}^2}{(p_0^2 + a^2 \vec{p}^2)(q_0^2 + a^2 \vec{q}^2)} \left[1 - \frac{(\vec{p} \cdot \vec{q})^2}{\vec{p}^2 \vec{q}^2} \right] \right\} \tag{4.33}
\end{aligned}$$

The details of performing the frequency sums in these expressions are discussed in the appendix and those sums needed for the components of the polarization tensor (4.30) to (4.33) also appear in the appendix.

4.2.1 The plasma parameters

We now look at the plasma parameters in the long wavelength, high temperature limit. In this limit, the equation for the transverse mode, (3.42), can be written as:

$$k_0^2 = \frac{1}{2} \Pi_{ii}^t \Big|_{\vec{k}^2=0} \tag{4.34}$$

For the longitudinal mode one can verify that the right-hand-side of Eq.(3.37) is negligible in the high temperature, long wavelength limit. As well, as happened for the covariant gauges, one finds that the term in (3.46) involving Φ of (4.30) vanishes in the high temperature, long wavelength limit, so that the longitudinal mode is obtained from

$$k_0^2 = \frac{k_i k_j \Pi^{ij}}{\vec{k}^2} \Big|_{\vec{k}^2=0} \tag{4.35}$$

Thus, in this limit the equations describing the transverse and longitudinal modes are the same as for the covariant gauges.

We first concentrate on the longitudinal mode. In the $\vec{k}^2 \rightarrow 0$ limit, one finds from (4.32) that

$$\begin{aligned} \frac{k_i k_j \Pi^{ij}}{\vec{k}^2} \Big|_{\vec{k}^2=0} &= -g^2 N \int dp \left[\frac{(1+z^2)}{p^2} + \frac{4\vec{p}^2 z^2}{p^2(q_0^2 - \vec{p}^2)} \right] \\ &- g^2 N \int dp \left[(1-z^2) \frac{[p_0^2 + a^2(\vec{p}^2 - 2p_0 k_0 + k_0^2)]}{p^2(q_0^2 + a^2\vec{p}^2)} \right] \\ &+ \frac{2a^2 z^2 k_0^2}{(p_0^2 + a^2\vec{p}^2)(q_0^2 + a^2\vec{p}^2)} \end{aligned} \quad (4.36)$$

where $z = \vec{p} \cdot \vec{k} / |\vec{p}| |\vec{k}|$. In the $\alpha \rightarrow 0$ limit, this expression agrees with that of Refs.[12, 13], who interpreted the ambiguous poles at $p_0 = 0$ using the principal value prescription. For finite α , however, the pole structure of (4.36) is unambiguous. One can now use the appropriate relations in the Appendix to do the frequency sums and carrying out the angular integrations, which leads then to the following expression for (4.36):

$$\begin{aligned} \frac{k_i k_j \Pi^{ij}}{\vec{k}^2} \Big|_{\vec{k}^2=0} &= g^2 N \frac{T^2}{9} + g^2 N \frac{k_0 T}{3\pi^2} \int_0^\infty dx \frac{1}{1 - 4x^2 + i\epsilon} \\ &- g^2 N \frac{k_0 T}{3\pi^2} \int_0^\infty dx \frac{2}{1 + 4a^2 x^2} \\ &+ g^2 N \frac{k_0 T}{3\pi^2} \int_0^\infty dx \frac{x^2(3 + 4a^2 + a^4) + a^2 - 1}{x^4(1 + a^2)^2 + 2x^2(a^2 - 1) + 1} \\ &- g^2 N \frac{k_0 T}{3\pi^2} \frac{1}{a^2} \int_0^\infty dx \frac{x^2(a^4 - 1) + 1 + 3a^2}{x^4(1 + a^2)^2 + 2x^2(a^2 - 1) + 1} \end{aligned} \quad (4.37)$$

It is necessary in (4.37) to keep $0 < \alpha < 1$, as otherwise the pole structure of the last three terms would not be determined. Within this range of α , the poles in these terms are found to lie off the real x axis.

In this form the computation of the bare one loop plasma parameters is straightforward. Consider first the determination of the plasma frequency ω_p from (3.50),

for which only the real parts of the terms in (4.37) are needed. One finds that to determine ω_p^2 to order g^2 only the first term in (4.37) is needed, the other terms being of order g^3 in the expansion and thus are negligible at this level. Therefore, at this level we find the usual result for the plasma frequency, $\omega_p^2 = g^2 NT^2/9$, independent of $0 < \alpha < 1$.

To determine the damping constant γ from (3.51) to this order, both the real and the imaginary parts of the expressions in (4.37) are needed. One finds first of all that for $0 < \alpha < 1$ only the second term in (4.37) contains an imaginary part. As for the contribution of the real parts of (4.37) to γ , one finds, as happened for ω_p , that only the first term in (4.37) is relevant to lowest order in g , the other terms being of higher order. Thus, we find to this order that the damping constant is given by $\gamma = g^2 NT/24\pi$, again independent of $0 < \alpha < 1$. This is the same result as found in calculations employing the principal value prescription in the timelike axial gauge [11, 12, 13], although as mentioned previously, no external prescription for handling ambiguous poles in the propagator need be imposed in the present formalism.

As we did for the covariant gauge calculation, it is interesting to compare the equations

$$k_0^2 = \frac{k_i k_j \Pi^{ij}}{\vec{k}^2} \Big|_{\vec{k}^2=0} \quad (4.38)$$

and

$$1 = \frac{\Pi_{00}}{\vec{k}^2} \Big|_{\vec{k}^2=0} + \frac{2\Phi}{k_0} \Big|_{\vec{k}^2=0} \quad (4.39)$$

to see the difference in employing $k^i k^j \Pi_{ij}$ as opposed to just Π_{00} in finding the plasma parameters. To do this, we calculate Φ of (4.30) in the high temperature,

long wavelength limit, and find it is given by

$$\begin{aligned} \frac{2\Phi}{k_0} \Big|_{\vec{k}^2=0} &= -\frac{1}{k_0^2} g^2 N \frac{k_0 T}{3\pi^2} \int_0^\infty dx \left\{ \frac{4}{1+4a^2x^2} \right. \\ &\quad \left. + \frac{2x^2(1+a^2)^2 + 2(a^2-1)}{x^4(1+a^2)^2 + 2x^2(a^2-1) + 1} \right\} \end{aligned} \quad (4.40)$$

One can show for $0 < \alpha < 1$ that Φ of (4.40) has no imaginary part. Furthermore, the contributions of its real part to the plasma parameters is of higher order than the level we are working at. Thus, to this order there is no difference in using (4.38) involving $k^i k^j \Pi_{ij}$ and in using (4.39) with only Π_{00} present, as the contribution of Φ is negligible. However, we know of no reason in principle why this should occur in this case; the fact that this is not so in the covariant gauges shows that it does not happen in general.

The α -independence of the plasma parameters to this order implies that the same parameters follow in the two interesting limiting cases : $\alpha \rightarrow 0$, corresponding to the static temporal gauge $\partial_0 A^0 = 0$, and for $\alpha \rightarrow 1$, corresponding to the Coulomb gauge $\partial_i A^i = 0$. This results, however, from taking the limits at the very end of the calculations. It is interesting to see what happens if the limits are taken at the level of the original four-dimensional integrals in (4.29). We have already mentioned that the $\alpha \rightarrow 0$ limit gives rise to ambiguous poles in the integrand at $p_0 = 0$, and thus an external prescription such as the principal value one must be used to define the integral. In the other limit of $\alpha \rightarrow 1$, one finds in doing the resulting integrals that curious terms proportional to $g^2 N |\vec{k}| T$ appear in the long wavelength, high temperature expansion [12, 13], which cause problems in determining the plasma parameters. The fact that problems arise can be seen by noticing that setting $\alpha = 1$ in the integrand of (4.37) results in an ill-defined expression. These problems were avoided in Refs. [12, 13] by considering the electric field correlation function, $\langle E^i E^j \rangle$,

rather than just the gluon propagator alone as has been done here. This resulted in the need for certain vertex corrections to be added to the equations for the plasma parameters determined by $\langle E^i E^j \rangle$ due to the fact that in the Coulomb gauge the electric correlation function and the gluon correlation function are not proportional, as they are in the timelike axial gauge. Including these corrections then yielded the same plasma parameters to this order as in the timelike axial gauge. It is interesting that with $0 < \alpha < 1$ in the present analysis no such vertex corrections are needed to get agreement between the temporal and Coulomb gauge results to this order when the limits are taken at the end of the calculation, while the corrections are needed if the Coulomb gauge limit is taken at the beginning. It would thus be instructive to see whether these vertex corrections contribute in the type of gauges considered here with the limit of the gauge parameter taken at the end.

We mention again that, while the plasma parameters are gauge parameter independent within this range of α to this order, this does not demonstrate gauge invariance of the final result for the damping constant, as higher loop graphs contributing to γ of the same order in $g^2 T$ must still be included. Therefore, the positive sign found for γ does not necessarily prove plasma stability. In this regard, we note that although we have assumed in the preceding analysis that $0 < \alpha < 1$ so that the parameter $a^2 = \alpha/(1 - \alpha)$ is positive, we can formally examine the results when a^2 becomes negative. In particular, consider Eq.(4.37) in the limit $a^2 \rightarrow -1$, (i.e., $\alpha \rightarrow \infty$), in which the bare propagator (4.28) corresponds to the Feynman gauge. In this limit the last three terms in (4.37) have ambiguous poles on the real x axis which, if interpreted using the $i\epsilon$ prescription, would pick up an imaginary part. One then finds in determining the plasma parameters that the plasma frequency ω_p^2 is unchanged to order g^2 , but the result for the damping constant γ to lowest order

is different. As one might expect, the γ so found agrees with that in the covariant gauge calculation (4.15) for the Feynman gauge, $\xi = 1$. We also note that Φ of (4.40) vanishes identically in the limit $a^2 \rightarrow -1$, as does the corresponding Φ of the covariant gauge, (4.9), for $\xi = 1$. This indicates that while Φ does not contribute to the determination of the plasma parameters to lowest order for $a^2 > 0$, it will for $a^2 < 0$ except in the limit $a^2 \rightarrow -1$, in analogy with the covariant gauges. As well, for negative a^2 we expect the damping constant to be gauge parameter dependent. These considerations show the importance of including the higher loop graphs in a fully self-consistent gauge invariant calculation.

We now turn to the calculation of the transverse plasma parameters from (4.34) in the high temperature, long wavelength limit, for which we need to calculate Π_{ii}^t . Having just found $k^i k^j \Pi_{ij}$ for the longitudinal mode, we thus have to find Π_{ii} of (4.33) in this limit. In the $\vec{k}^2 \rightarrow 0$ limit, one has

$$\begin{aligned} \Pi_{ii}(k)|_{\vec{k}^2=0} &= -g^2 N \int dp \left\{ \frac{4}{p^2} + \frac{4\vec{p}^2}{p^2(q_0^2 - \vec{p}^2)} \right. \\ &\quad \left. + \frac{2[p_0^2 + a^2(k_0^2 - 2p_0 k_0 + \vec{p}^2)]}{p^2(q_0^2 + a^2\vec{p}^2)} + \frac{2a^2 k_0^2}{(p_0^2 + a^2\vec{p}^2)(q_0^2 + a^2\vec{p}^2)} \right\} \end{aligned} \quad (4.41)$$

Performing the frequency sums and doing the angular integrations leads then to the general result of (4.13),

$$\Pi_{ii}|_{\vec{k}^2=0} = 3 \frac{k_i k_j \Pi^{ij}}{\vec{k}^2} \Big|_{\vec{k}^2=0} \quad (4.42)$$

in the high temperature limit, where $k^i k^j \Pi_{ij}$ appears in (4.37). Thus, in this limit, the transverse and longitudinal plasma frequency and damping constant are the same to this order, as one expects. In addition, similar conclusions concerning the relative contribution of Φ to the transverse equation can be made as was done for the longitudinal one.

4.2.2 The static limit

In the static limit one finds, the equation for the transverse pole (3.42) is

$$\vec{k}^2 = -\frac{1}{2}\Pi_{ii}\Big|_{k_0=0} \quad (4.43)$$

For the longitudinal mode, one finds from (4.27) that the right-hand-side of (3.37) is negligible in the static limit. As well, since Φ of (4.30) vanishes in the $k_0 = 0$ limit, from (3.46) the equation becomes

$$\vec{k}^2 = \Pi_{00}|_{k_0=0} \quad (4.44)$$

Thus, as happened for the plasma parameters, the equations describing the two modes in this limit are the same as those for the covariant gauge.

We first look at the longitudinal mode, for which Π_{00} is required. One finds from (4.31) that in the static limit

$$\begin{aligned} \Pi_{00}|_{k_0=0} &= \frac{1}{2}g^2 N \int dp \left\{ \frac{4(2c^2 - 1)}{p^2} + \frac{4(1 - c^2)}{(p_0^2 + a^2\vec{p}^2)} \right. \\ &\quad \left. - \frac{2a^2[\vec{k}^2 + 2\vec{p} \cdot \vec{q} + c^2(\vec{k}^2 - 2\vec{p} \cdot \vec{q})]}{(p_0^2 + a^2\vec{p}^2)(p_0^2 + a^2\vec{q}^2)} - \frac{4p_0^2(1 + c^2)}{p^2(p_0^2 - \vec{q}^2)} \right\} \end{aligned} \quad (4.45)$$

where $c = \vec{p} \cdot \vec{q} / |\vec{p}| |\vec{q}|$. Doing the frequency sums and angular integrations leads to, in the high temperature, long wavelength limit, the following result.

$$\begin{aligned} \Pi_{00}|_{k_0=0} &= -\frac{1}{3}g^2 NT^2 + \frac{g^2 N |\vec{k}| T}{4\pi^2} \int_0^\infty dx \left\{ \frac{2}{x} \ln \left| \frac{1+x}{1-x} \right| \right. \\ &\quad \left. + \left[3 + \frac{2}{a^2} \right] \left[2 - x \ln \left| \frac{1+x}{1-x} \right| \right] \right\} \\ &= -\frac{1}{3}g^2 NT^2 + \frac{1}{4}g^2 N |\vec{k}| T \end{aligned} \quad (4.46)$$

This results in Eq.(4.44) for the longitudinal pole becoming

$$\vec{k}^2 + \frac{1}{3}g^2 NT^2 - \frac{1}{4}g^2 N |\vec{k}| T = 0 \quad (4.47)$$

which is the same as that found for the covariant gauges, (4.21).

For the transverse pole, we need Π_{ii} of (4.33) in the static limit. One finds

$$\begin{aligned} \Pi_{ii}|_{k_0=0} &= -\frac{1}{2}g^2 N \int dp \left\{ \frac{8}{p^2} + \frac{2(2-3a^2)}{(p_0^2 + a^2\vec{p}^2)} \right. \\ &+ \frac{1}{p^2(p_0^2 - \vec{q}^2)} [9\vec{k}^2 - 20\vec{p} \cdot \vec{q} - 7c^2\vec{k}^2 + 12c^2\vec{p} \cdot \vec{q}] \\ &+ \frac{2}{p^2(p_0^2 + a^2\vec{q}^2)} [2a^2p_0^2 + \vec{k}^2 + 4\vec{p} \cdot \vec{q} + 6c^2\vec{p}^2 + c^2\vec{k}^2] \\ &\left. + \frac{1}{(p_0^2 + a^2\vec{p}^2)(p_0^2 + a^2\vec{q}^2)} [a^4(\vec{k}^2 - 2\vec{p} \cdot \vec{q}) + 2a^2p_0^2 + (1-c^2)\vec{k}^2] \right\} \end{aligned} \quad (4.48)$$

where c is defined as in (4.45). In the high temperature, long wavelength limit, we find this expression becomes

$$\begin{aligned} \Pi_{ii}|_{k_0=0} &= -\frac{g^2 N |\vec{k}| T}{8\pi^2} \int_0^\infty dx \left\{ \frac{10}{x} \ln \left| \frac{1+x}{1-x} \right| \right. \\ &- \frac{1}{x} \left(\frac{11}{4} + \frac{1}{2a^2} - \frac{1}{4a^4} \right) \left[\ln \left| \frac{x^2(1+a^2) + 4x + 4}{x^2(1+a^2) - 4x + 4} \right| \right. \\ &\left. \left. + \ln \left| \frac{x^2(1+a^2) + 4a^2x + 4a^2}{x^2(1+a^2) - 4a^2x + 4a^2} \right| \right] \right\} \\ &= -\frac{1}{32a^4} (9a^4 - 2a^2 + 1) g^2 N |\vec{k}| T \end{aligned} \quad (4.49)$$

The equation for the transverse pole, (4.43), then becomes

$$\vec{k}^2 - \frac{1}{64a^4} (9a^4 - 2a^2 + 1) g^2 N |\vec{k}| T = 0 \quad (4.50)$$

which, as for the covariant gauges, (4.20), has the Landau ghost problem [59]. There are two interesting properties of this result. The first is that, while the first term

in the first relation in (4.49) gives the result of the timelike axial gauge using the principal value prescription [11], the final result of (4.50) is singular in the $\alpha \rightarrow 0$ limit. This singularity is connected to the second feature that if one compares (4.50) with the covariant gauge result (4.20), one finds the equations are the same if the formal identification

$$a^2 = \frac{\alpha}{(1-\alpha)} \leftrightarrow -\frac{1}{\xi} \quad (4.51)$$

is made. Thus, the $\alpha \rightarrow 0$ limit corresponds in this sense to the $\xi \rightarrow \infty$ limit, which is also singular for the covariant gauge result. The reason for the correspondence (4.51) between this and the covariant gauge is simple : if one compares the static gauge propagator (4.28) with the covariant gauge propagator (4.5), one sees that at $k_0 = 0$ the respective gauge parameters are related as in (4.51). Since in the high temperature, long wavelength limit the leading term in the frequency sum is $n = 0$, $\Pi_{ii}(k_0 = 0)$ of (4.48) corresponds directly in this limit to that of the covariant gauge with the identification (4.51) made.

It is not known what implications these results may have for the temporal gauge calculation using the principal value prescription of the static poles [11], as in a sense α here could be viewed as a regulating parameters used to define ambiguous integrals at $\alpha = 0$. It is curious then that the $\alpha \rightarrow 0$ limit reproduces the plasma parameters found using the principal value prescription as well as the longitudinal static pole, but is a singular limit for the transverse static pole. Perhaps related to this, it is also curious that the same plasma parameters and longitudinal static pole are found as those [11, 12, 13] calculated using the electric field correlation function $\langle E^i E^j \rangle$ in the temporal gauge with the principle value prescription, but the transverse static pole is different than that found [19] using the magnetic field correlation function

$\langle B^i B^j \rangle$ and its corresponding vertex corrections, again in the temporal gauge with the principle value prescription. As before, it would be interesting to see what these vertex corrections contribute in the class of gauges considered here.

4.3 Conclusions

The foregoing analysis illustrates some important technical aspects of the calculation of physical poles in the gluon propagator in gauges where the polarization tensor is not transverse perturbatively. Two classes of such gauges were discussed in detail: the covariant gauge and a one-parameter family of non-covariant gauges which interpolates between the static temporal gauge and the Coulomb gauge. It was shown that the equations describing the response of the transverse and longitudinal gluon modes do in principle contain contributions from the longitudinal part of the self-energy, but that a Ward identity could be used to show that these contributions vanish in the long-wavelength high temperature limit in the class of gauges considered here. There are nonetheless important differences between the equations derived here and those normally used for transverse self-energies.

A number of interesting results emerged from our analysis of the plasma parameters and of the Landau ghosts in the family of non-covariant gauges. The one-loop damping constant was shown to be independent of the gauge fixing parameter for $0 < \alpha < 1$ and equal to the result obtained in the temporal gauge using the principal value prescription. Moreover, since the $\alpha \rightarrow 0$ limit corresponds to the static temporal gauge and $\alpha \rightarrow 1$ to the Coulomb gauge, the present formalism yields the same one loop plasma parameters in the Coulomb gauge as in the static temporal gauge,

without the use of vertex corrections as needed in Ref.[13] in the consideration of the electric field correlation function with the $\alpha \rightarrow 1$ limit taken at the beginning. In addition, if one formally examines the $\alpha \rightarrow \infty$ limit, the one loop damping constant of the ordinary Feynman gauge is reproduced, and in general for $\alpha > 1$ we expect γ to be gauge parameter dependent. With regard to the Landau ghosts, the present calculations illustrate a correspondence between the location of these poles in the family of non-covariant gauges considered here and those obtained in the covariant gauge. Moreover, the $\alpha \rightarrow 0$ limit reproduces the longitudinal timelike axial gauge Landau ghost obtained using the principal value prescription, but is a singular limit for the transverse Landau ghost. In this case a difference does arise between using just the gluon propagator and the magnetic field correlation function in the temporal gauge using the principal value prescription.

It must of course be stressed that a consistent approximation scheme for calculating the damping constant and the Landau ghosts must be made, requiring for example the inclusion of higher loop diagrams for the damping constant as described by Pisarski [22, 23] which will be done in the next chapter, or the considerations of Elze *et al* in Ref.[19] for the Landau ghosts. In this regard, the gauge invariant propagator of Cornwall [60, 61] may also be worth considering, although as argued by Pisarski [23], this may be more a matter of convenience rather than one of necessity. In any case, one cannot as yet ascribe any physical importance to the numerical results obtained in the present paper, nor to the apparent gauge fixing independence for $0 < \alpha < 1$ of the one loop damping constant in the family of non-covariant gauges.

Chapter 5

Resummation

The only physically meaningful calculations in gauge theories are those which satisfy the requirements of gauge invariance and self consistency. It is known that a determination of γ at the one-loop level cannot be fully consistent due to the infrared behaviour of the theory, since there are most probably corrections from two-loop and higher order diagrams which contribute to the term $\sim g^2 T$ [62, 12, 13]. Physically speaking, the decay of a massive perturbation in the plasma into two bare transverse gluons with $\omega = |\mathbf{k}|$ should be replaced by a decay into dressed gluons with a medium-induced effective mass and a modified dispersion relation $\omega(k)$. This can, of course, entirely change the value of γ , although not its sign. The question whether the discrepancies found by various groups at the one-loop level can or cannot be explained by invoking the above consistency argument was unsettled. Some argued that a unique result will be obtained if one knows how to subject the system in each case to the same physical perturbation and calculate the same physical response. Some others suggested that γ should be defined in terms of some more complicated,

but gauge invariant way, as, for instance, the gauge invariant propagator of Cornwall [60, 61]. Pisarski, in particular, suggests that it does not matter what is used to compute the plasmon's pole, but how it is computed. General formal arguments also exist to support the conclusion that the poles in the propagator will be gauge invariant when calculated accurately [27]. In this chapter, the Braaten and Pisarski resummation techniques will be used to calculate the damping rate for both heavy and massless fermions in the long wavelength limit [34].

5.1 Hard thermal loops and effective propagators and vertices

For hot field theories two natural momentum scales arise; one is of the order of T , which is called "hard", and the other is of the order of gT , which is termed "soft". The definition of terms $\sim gT$ is, loosely speaking, things which are powers of gT , with no g 's left over. Thus, terms $\sim gT, \sim (gT)^2, \sim (gT)^3, \dots$ are of the same order and should be added together. For hot gauge theories we term the diagrams which must be resummed into effective propagators and vertices "hard thermal loops". When any external leg is hard, these diagrams are at least g times the tree amplitude and are part of the usual perturbative corrections. When every external momentum is soft, hard thermal loops are of the same order as the tree diagrams and in principle must be incorporated into the tree diagrams. The interesting thing is that not only are they given merely by diagrams at one-loop order, but by a small subset of the complete one-loop diagram, when the virtual momenta within the diagram is hard, $\sim T$.

5.1.1 Gluon propagator

Hard thermal loops are generated solely by a small part of the integration region in one-loop diagrams in which the loop momentum is hard. Therefore, compared to the loop momentum, all the soft external momenta which appear in the numerator can be neglected, for instance, the k 's appear in the integrand of Eq.(4.8). Thus, the hard thermal loop contribution to the soft gluon polarization tensor in the usual covariant gauge can be obtained from (4.8) by setting $k = 0$ at the numerator and one gets:

$$\begin{aligned} \delta\Pi_{\mu\nu} &\approx g^2 N \int dp \left[\frac{2g_{\mu\nu}}{Q^2} - \frac{4p_\mu p_\nu}{P^2 Q^2} \right] \\ &\approx -3m_g^2 \left[n_\mu n_\nu - n \cdot k \left\langle \frac{\hat{P}_\mu \hat{P}_\nu}{K \cdot \hat{P}} \right\rangle \right] \end{aligned} \quad (5.1)$$

which is independent of the gauge parameter ξ and turns out to be gauge independence. Here, $\hat{P}^\mu = (1, \hat{\mathbf{p}} = \mathbf{p}/|\mathbf{p}|)$ and $\langle \dots \rangle$ denotes an average over the directions $\hat{\mathbf{p}}$, and the so called thermal mass m_g is given by $m_g^2 = g^2 T^2 (N + \frac{1}{2} N_f)/9$ for N_f flavours of massless fermions. In this and the following ' \approx ' denotes equality up to hard thermal loop contributions. The gauge invariance of high temperature limiting values (which are proportional to T^2) is easily proved by noticing that for the polarization tensor the terms of order T^2 come only from structures quadratically divergent in the ultraviolet region while the gauge dependent longitudinal parts of the propagators do not contain such structures.

It can be easily verified that the above polarization tensor is transverse, i.e. $k^\mu \delta\Pi_{\mu\nu} \approx 0$, and hence the coefficients of the corresponding longitudinal components vanish, $\Lambda, \Phi \approx 0$. Besides the transversality, one should realize that the effect of the hard thermal loops is of the same order as the soft tree level diagram, $\sim (gT)^2$.

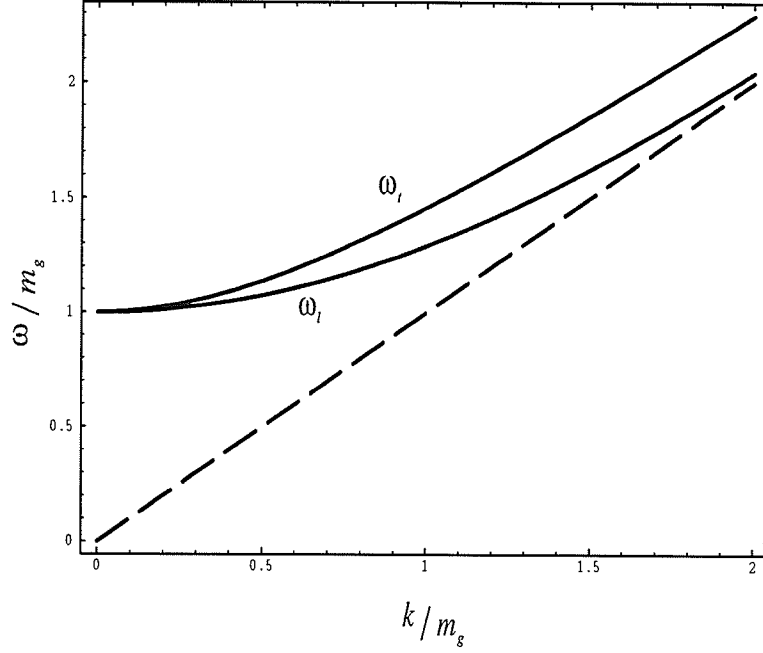


Figure 5.1: Gluon excitations at non-zero temperature

Therefore, for a Feynman diagram containing some soft bare gluon propagators, one has to sum all the hard thermal loops effects, $\delta\Pi_{\mu\nu}$, to the bare propagators via the Dyson's equation. In contrast, a self energy insertion in the usual low temperature case (by that we means $(gT)^4/(gT)^2 \approx g^2$) will at least decrease the order of magnitude of the corresponding Feynman diagram by g^2 and hence contribute to a higher loop series expansion.

One can formally use the methods develop in chapter 3 to incorporate the hard thermal loops effect into an effective propagator. Eq.(3.30) can be simplified by

using the transversality into the following forms:

$$k_t^2 = K^2 + \Pi, \quad (5.2a)$$

$$\gamma = C_{(0)}, \quad (5.2b)$$

$$\delta = D_{(0)}, \quad (5.2c)$$

$$\mathbf{k}_l^2 = K^2 + \chi. \quad (5.2d)$$

By substituting these into (3.14), the effective gluon propagator is given by

$$D_{\mu\nu}(k) = \frac{1}{k_t^2} A_{\mu\nu} - \frac{1}{k_l^2} \mathcal{F}^\mu \mathcal{F}^\nu + c^2(k) \frac{k^\mu k^\nu}{k^4} \quad (5.3)$$

where $k_l^2 \equiv \vec{k}^2 k_l^2 / K^2$. For convenience sake, we write from now on $1/C_{(0)} = c^2$ and $D_{(0)} = \lambda$. Strightforward calculations show

$$\begin{aligned} \Pi(k_0, k) &\approx -\frac{3m_g^2 k_0^2}{2k^2} \left[1 - \left(1 - \frac{k^2}{k_0^2} \right) \frac{k_0}{2k} \ln \left(\frac{k_0 + k}{k_0 - k} \right) \right], \\ \Pi_l(k_0, k) &\approx -3m_g^2 \left[1 - \frac{k_0}{2k} \ln \left(\frac{k_0 + k}{k_0 - k} \right) \right] \end{aligned} \quad (5.4)$$

where $\Pi_l = -\vec{k}^2 \chi / K^2$. By solving the transverse and the plasmon dispersion relations $k_{t,l}^2[\omega_{t,l}(k), k] = 0$ [63, 28] analytically, one obtains the following limiting forms of the quasiparticle excitations:

$$\omega_t(k) \stackrel{k \rightarrow 0}{\approx} m_g + \frac{3}{5} \frac{k^2}{m_g} - \frac{9}{35} \frac{k^4}{m_g^3} + \dots, \quad (5.5a)$$

$$\omega_t(k) \stackrel{k \rightarrow \infty}{\approx} k + \frac{3m_g^2}{4k} - \frac{9}{32} \frac{m_g^4}{k^3} \left(2 \log \left(\frac{8}{3} \frac{k^2}{m_g^2} \right) - 3 \right) + \dots, \quad (5.5b)$$

$$\omega_l(k) \stackrel{k \rightarrow 0}{\approx} m_g + \frac{3}{10} \frac{k^2}{m_g} - \frac{3}{280} \frac{k^4}{m_g^3} + \dots, \quad (5.5c)$$

$$\omega_l(k) \stackrel{k \rightarrow \infty}{\approx} k \left(1 + 2x_l + \left(\frac{8}{3} \frac{k^2}{m_g^2} + 10 \right) x_l^2 + \dots \right) \quad (5.5d)$$

where $x_l = \exp\left[-\frac{2k^2}{3m_g^2} - 2\right]$. The transverse pole represents the usual transverse excitations of a gauge field, renormalized by temperature to lie above the light cone by $\sim m_g$. The longitudinal pole on the other hand behaves like a massive excitation only about zero momentum and its mass shell is exponentially close to the light cone at large momentum. The dispersion equations can also be solved by numerical method and the results are displayed in Fig. 5.1.

Define the spectral densities by the following equation:

$$\frac{1}{k_{t,l}^2} = \int \frac{d\omega}{2\pi} \frac{\rho_{t,l}(\omega, k)}{(k_0 - \omega)}. \quad (5.6)$$

One obtains

$$\begin{aligned} & \rho_t(k_0, k) \\ = & 2\pi \Im \frac{1}{k_t^2} \\ = & 2\pi R_t(k_0, k) [\delta(k_0 - \omega_t(k)) - \delta(k_0 + \omega_t(k))] + 2\pi \beta_t(k_0, k) \theta(k^2 - k_0^2) \end{aligned} \quad (5.7)$$

and

$$\begin{aligned} & \frac{K^2}{2\pi k^2} \rho_l(k_0, k) \\ = & \Im \frac{1}{k_l^2} \\ = & R_l(k_0, k) [\delta(k_0 - \omega_l(k)) - \delta(k_0 + \omega_l(k))] + \beta_l(k_0, k) \theta(k^2 - k_0^2). \end{aligned} \quad (5.8)$$

Without much difficulty, one can derive

$$R_t(\omega, k) = \frac{\omega(\omega^2 - k^2)}{3m_g^2\omega^2 - (\omega^2 - k^2)^2},$$

$$\begin{aligned}
R_l(\omega, k) &= \frac{\omega(\omega^2 - k^2)}{k^2(3m_g^2 - \omega^2 + k^2)}, \\
\beta_t(\omega, k) &= \frac{1}{\pi} \frac{\Pi^I}{(k^2 - \omega^2 - \Pi^R)^2 + (\Pi^I)^2}, \\
\beta_l(\omega, k) &= -\frac{1}{\pi} \frac{\Pi_l^I}{(k^2 - \Pi_l^R)^2 + (\Pi_l^I)^2}
\end{aligned} \tag{5.9}$$

and

$$\begin{aligned}
\Pi^I(\omega, k) &= \frac{3\pi m_g^2 \omega (k^2 - \omega^2)}{4k^3}, \\
\Pi_l^I(\omega, k) &= -\frac{3\pi m_g^2 \omega}{2k}, \\
\Pi^R(\omega, k) &= -\frac{3m_g^2 \omega^2}{2k^2} \left[1 + \left(\frac{k^2}{\omega^2} - 1 \right) \frac{\omega}{2k} \ln \left(\frac{k + \omega}{k - \omega} \right) \right], \\
\Pi_l^R(\omega, k) &= -3m_g^2 \left[1 - \frac{\omega}{2k} \ln \left(\frac{k + \omega}{k - \omega} \right) \right].
\end{aligned} \tag{5.10}$$

Besides the contribution from poles to the spectral densities, due to Landau damping, the logarithmic functions in Π and Π_l acquire imaginary parts for $k_0 = k$ down to $k_0 = 0$, which contribute to $\rho_{t,l} \neq 0$ below the light cone.

5.1.2 Quark propagator

The effective propagator for massless quark $*S^{-1}(P) = \not{P} - \delta\Sigma(P)$ includes the hard thermal loop [64, 65]

$$\begin{aligned}
\delta\Sigma(P) &\approx g^2 C_f \int dK D_{\mu\nu}^{(0)}(K) \gamma^\mu S^{(0)}(P - K) \gamma^\nu \\
&\approx m_f^2 \gamma_\mu \left\langle \frac{\hat{K}^\mu}{P \cdot \hat{K}} \right\rangle \equiv \gamma_\mu \xi^\mu(P).
\end{aligned} \tag{5.11}$$

Here, $m_f^2 = C_f g^2 T^2 / 8$ is the radiatively induced fermion “mass” and C_f is the quadratic Casimir eigenvalue for the fermions. $D_{\mu\nu}^{(0)}(P)$ is the bare gluon propagator

and $S^{(0)}(P) = (\not{P} - m)^{-1}$ is the bare quark propagator with mass m in general. Now, $P \cdot \xi = m_f^2$ from Eq.(5.11) gives $\xi^i(P) = [p_0 \xi_0 - m_f^2] \hat{p}^i / p$, which as shown in Refs.[64, 65] can be used to split the effective propagator into two modes :

$$\begin{aligned} {}^*S(P) &= \frac{1}{D_0(P)\gamma^0 - D_s(P)\not{p}} = \chi_0(P)\gamma_0 - \chi_s(P)\not{p} \\ &= \frac{1}{2}\Delta_+(P)[\gamma_0 - \not{p}] + \frac{1}{2}\Delta_-(P)[\gamma_0 + \not{p}], \end{aligned} \quad (5.12)$$

where

$$\begin{aligned} D_0(P) &= p_0 - \xi_0, \\ D_s(P) &= p - \frac{p_0 \xi_0 - m_f^2}{p}, \\ \Delta_+(P) &= \frac{1}{D_0(P) - D_s(P)}, \\ \Delta_-(P) &= \frac{1}{D_0(P) + D_s(P)}. \end{aligned} \quad (5.13)$$

The dispersion relations of these two modes and their spectral densities are discussed in Refs.[64, 65].

On mass shell, spinors satisfy $D_0(P)\gamma^0\psi = D_s(P)\not{p}\psi$ or equivalently

$$\gamma^5\psi = \frac{D_s}{D_0}\not{p} \cdot \Sigma\psi$$

where $\hat{p} \cdot \Sigma = \gamma^5\gamma^0\not{p}$ is the helicity operator. At zero temperature, $D_0 = p_0$ and $D_s = p$, which means helicity is equal to chirality for all positive energy states. At finite temperature, instead of one there are two possible modes of excitation; $D_0 = D_s$ with the usual relation between helicity and chirality as at zero temperature, and $D_0 = -D_s$ with a flipped helicity. The dispersion relations

$$\begin{aligned} \omega_+ &= p + \frac{m_f^2}{p} \left[1 + \frac{1}{2} \left(1 - \frac{\omega_+}{p} \right) \ln \left(\frac{\omega_+ + p}{\omega_+ - p} \right) \right], \\ \omega_- &= -p + \frac{m_f^2}{p} \left[-1 + \frac{1}{2} \left(1 + \frac{\omega_-}{p} \right) \ln \left(\frac{\omega_- + p}{\omega_- - p} \right) \right] \end{aligned} \quad (5.14)$$

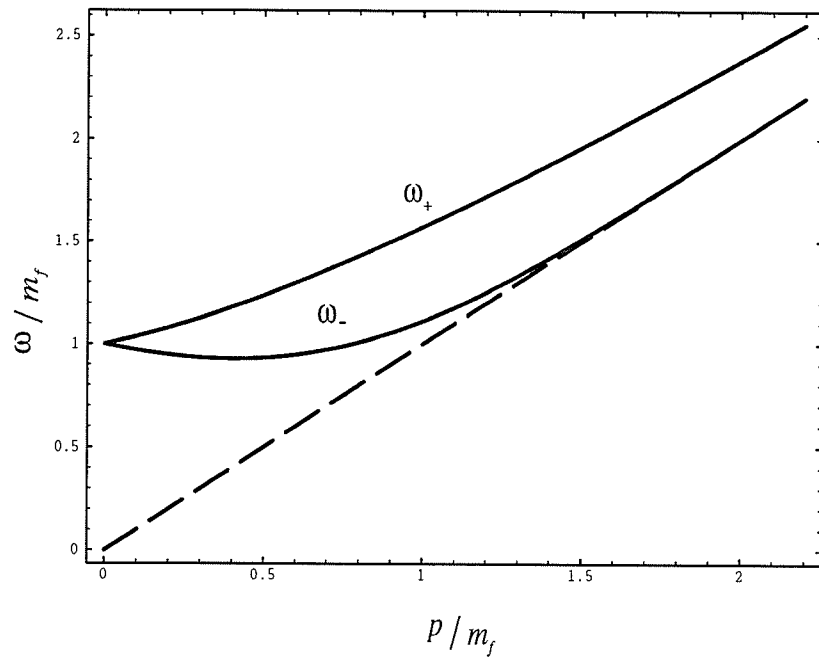


Figure 5.2: Fermion excitations at non-zero temperature

can be solved both analytically for some limiting cases and numerically as in Fig. 5.2.

$$\omega_+(p) \stackrel{p \rightarrow 0}{\approx} m_f + \frac{p}{3} + \dots, \quad (5.15a)$$

$$\omega_+(p) \stackrel{p \rightarrow \infty}{\approx} p + \frac{m_f^2}{p} + \dots, \quad (5.15b)$$

$$\omega_-(p) \stackrel{p \rightarrow 0}{\approx} m_f - \frac{p}{3} + \dots, \quad (5.15c)$$

$$\omega_-(p) \stackrel{p \rightarrow \infty}{\approx} p(1 + 2x + 4x^2 + \dots) \quad (5.15d)$$

where $x = \exp(-2\vec{p}^2/m_f^2 - 1)$.

$$\Im_p \Delta_+(p_0, p) = R(p_0, p) [\delta(p_0 - \omega_+(p)) + \delta(p_0 + \omega_-(p))] + \beta_+(p_0, p) \theta(p^2 - p_0^2),$$

$$\Im_p \Delta_-(p_0, p) = R(p_0, p) [\delta(p_0 - \omega_-(p)) + \delta(p_0 + \omega_+(p))] + \beta_-(p_0, p) \theta(p^2 - p_0^2),$$

(5.16)

$$R(\omega, p) = \frac{\omega^2 - p^2}{2m_f^2},$$

$$\beta_+(\omega, p) = \frac{1}{\pi} \frac{D_0^I - D_s^I}{(D_0^R - D_s^R)^2 + (D_0^I - D_s^I)^2},$$

$$\beta_-(\omega, p) = \beta_+(-\omega, p),$$

$$D_0^I(p) = \frac{\pi m_f^2}{2p},$$

$$D_s^I(\omega, p) = \frac{\pi m_f^2 \omega}{2p^2},$$

$$D_0^R(\omega, p) = \omega - \frac{m_f^2}{2p} \ln \left(\frac{p + \omega}{p - \omega} \right),$$

$$D_s(\omega, p) = p - \frac{m_f^2}{p} \left[\frac{\omega}{2p} \ln \left(\frac{p + \omega}{p - \omega} \right) - 1 \right], \quad (5.17)$$

5.1.3 Three-point vertex

The effective vertex between a quark pair and a gluon is illustrated in Fig. 5.3. The effective quark-gluon vertex can be decomposed into the following:

$$*\Gamma^\mu(P, Q) = \gamma^\mu + \delta\Gamma_{(1)}^\mu + \delta\Gamma_{(2)}^\mu \equiv \gamma^\mu + \delta\Gamma^\mu(P, Q), \quad (5.18)$$

where P and Q are the incoming and outgoing quark momenta respectively. The two hard thermal loops are given by

$$\begin{aligned} \delta\Gamma_{(1)}^\mu(P, Q) &\approx g^2 \left[C_f - \frac{C}{2} \right] \int dK D_{\lambda\rho}^{(0)}(K) \gamma^\rho S^{(0)}(P - K) \gamma^\mu S^{(0)}(Q - K) \gamma^\lambda, \\ \delta\Gamma_{(2)}^\mu(P, Q) &\approx -\frac{g^2 C}{2} \int dK \gamma^\beta S^{(0)}(K) \gamma^\rho D_{\rho\nu}^{(0)}(K - P) \times \\ &\quad \Gamma^{\mu\nu\alpha}(P - Q, K - P, Q - K) D_{\alpha\beta}^{(0)}(K - Q), \end{aligned} \quad (5.19)$$

where $\Gamma^{\alpha\beta\gamma}(P, Q, K) = g^{\alpha\beta}(P - Q)^\gamma + g^{\beta\gamma}(Q - K)^\alpha + g^{\gamma\alpha}(K - P)^\beta$ and C is the Casimir eigenvalue of the adjoint representation. $\delta\Gamma_{(1)}^\mu$ is an abelian graph except for the group-theoretic weight factor. It turns out that the terms proportional to $N/2$ cancel, and we have [29, 30, 31]

$$\delta\Gamma^\nu(P, Q) \approx m_f^2 \gamma_\mu \left\langle \frac{\hat{K}^\mu \hat{K}^\nu}{P \cdot \hat{K} Q \cdot \hat{K}} \right\rangle, \quad (5.20)$$

which, using the effective quark propagator of Eq.(5.11), gives the Ward identity

$$(Q - P) \cdot *\Gamma(P, Q) \approx *S^{-1}(Q) - *S^{-1}(P). \quad (5.21)$$

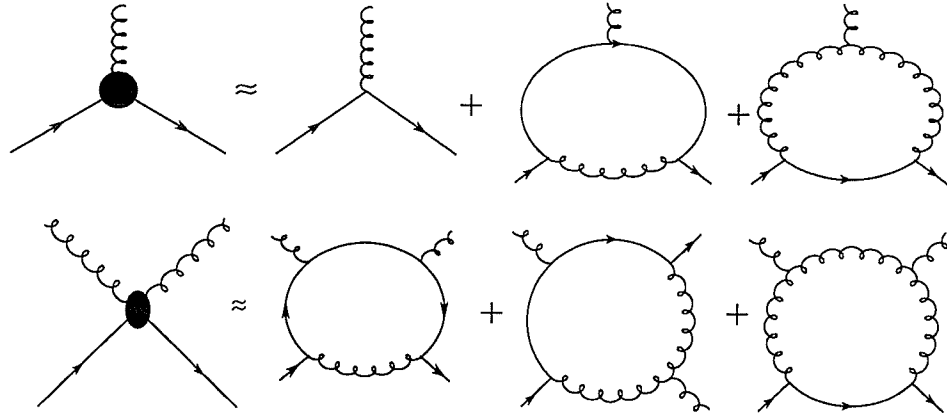


Figure 5.3: The effective vertices: (a) ${}^*\Gamma^\mu$ between a quark pair and a gluon, (b) ${}^*\Gamma^{\mu\nu}$ between a quark pair and two gluons.

5.1.4 Four-point vertex

The effective four-point vertex between a quark pair and two gluons is illustrated in Fig. 5.3. Since there is no bare vertex, the effective vertex is completely given by the hard thermal loop. With the colour indices contracted,

$${}^*\Gamma^{\mu\nu}(P, Q; S, T) = \delta\Gamma_{(1)}^{\mu\nu} + \delta\Gamma_{(2)}^{\mu\nu} + \delta\Gamma_{(3)}^{\mu\nu} \quad (5.22)$$

where $P + S = Q + T = R$. The three hard thermal loops are decomposed as

$$\delta\Gamma_{(i)}^{\mu\nu}(P, Q; S, T) = \mathcal{J}_{(i)}^{\mu\nu}(P, Q; S, T) + \mathcal{J}_{(i)}^{\mu\nu}(P, Q; -T, -S) \quad (5.23)$$

for $i = 1, 2, 3$ indicating the number of internal gluon propagators, where

$$\begin{aligned} & \mathcal{J}_{(1)}^{\mu\nu}(P, Q; S, T) \\ & \approx g^2 C_f \int dK \gamma^\lambda S^{(0)}(Q + K) \gamma^\nu S^{(0)}(R + K) \gamma^\mu S^{(0)}(P + K) \gamma^\rho D_{\rho\lambda}^{(0)}(K), \\ & \approx m_f^2 \gamma_\rho \left\langle \frac{\hat{K}^\mu \hat{K}^\nu \hat{K}^\rho}{P \cdot \hat{K} (P + S) \cdot \hat{K} Q \cdot \hat{K}} \right\rangle, \end{aligned} \quad (5.24)$$

$$\begin{aligned}
& \mathcal{J}_{(2)}^{\mu\nu}(P, Q; S, T) \\
& \approx \frac{g^2 N}{2} \int dK D_{\alpha\beta}^{(0)}(K+S) \gamma^\beta S^{(0)}(Q-S-K) \gamma^\nu S^{(0)}(P-K) \gamma^\lambda \times \\
& \quad \times D_{\lambda\rho}^{(0)}(K) \Gamma^{\rho\mu\alpha}(K, S, -K-S), \\
& \approx -\frac{C}{2C_f} m_f^2 \gamma_\rho \left\langle \frac{\hat{K}^\mu \hat{K}^\nu \hat{K}^\rho}{(P-T) \cdot \hat{K} (P+S) \cdot \hat{K}} \right\rangle \left(\frac{1}{P \cdot \hat{K}} + \frac{1}{Q \cdot \hat{K}} \right), \quad (5.25)
\end{aligned}$$

$$\begin{aligned}
& \mathcal{J}_{(3)}^{\mu\nu}(P, Q; S, T) \\
& \approx g^2 N \int dK D_{\alpha\beta}^{(0)}(K) \Gamma^{\mu\beta\gamma}(-S, K, S-K) D_{\gamma\delta}^{(0)}(S-K) \times \\
& \quad \times \Gamma^{\nu\delta\rho}(T, K-S, Q-P-K) D_{\rho\lambda}^{(0)}(Q-K-P) \gamma^\lambda S^{(0)}(P+K) \gamma^\alpha \\
& \approx \frac{C}{C_f} \mathcal{J}_{(1)}^{\mu\nu}(P, Q; S, T). \quad (5.26)
\end{aligned}$$

It can be easily verified that $\delta\Gamma_{(2)}^{\mu\nu}$ and $\delta\Gamma_{(3)}^{\mu\nu}$ cancel, and we have [29, 30, 31]

$${}^* \Gamma^{\mu\nu}(P, Q; S, T) \approx m_f^2 \gamma_\rho \left\langle \frac{\hat{K}^\mu \hat{K}^\nu \hat{K}^\rho}{(P+S) \cdot \hat{K} (P-T) \cdot \hat{K}} \left[\frac{1}{P \cdot \hat{K}} + \frac{1}{Q \cdot \hat{K}} \right] \right\rangle, \quad (5.27)$$

which, using the 3-point vertex of Eq.(5.20), leads to the Ward identity

$$T_\mu {}^* \Gamma^{\mu\nu}(P, Q; S, T) \approx {}^* \Gamma^\nu(P-T, Q) - {}^* \Gamma^\nu(P, Q+T). \quad (5.28)$$

5.2 Resummation

The essence of the resummation methods, perhaps, is the recognition of the differences between effects that are of order $\sim gT$, and those that are g times terms $\sim gT$. For example, $\delta\Sigma$ is real above the light cone. In order to include the leading order contribution to the imaginary part of the self energy with soft on shell fermions, one has to add to the Dyson's equation the so called effective or resummed self energy

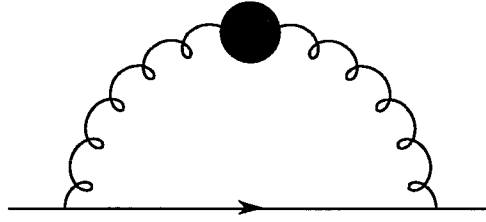


Figure 5.4: Resummed fermion propagator

$^*\Sigma$ which incorporates all effects up to $\sim g^2 T$. Therefore, for a massless fermion, we have, up to $\sim g^2 T$,

$$S^{-1}(P) = \not{P} - \delta\Sigma(P) - ^*\Sigma(P). \quad (5.29)$$

5.2.1 Heavy quark

Employing dispersion relation methods, Pisarski has used the effective expansion to calculate the lowest order damping rate of a heavy quark of mass $m \gg T$ in the long wavelength limit [64]. We reconsider this calculation as a simple check on the methods of Appendix A. With $m \gg T$ only the bare gluon propagator has to be replaced by its effective form, which leads to consideration of the resummed self-energy [64]

$$^*\Sigma(P) = g^2 C_f \int_{soft} dK D_{\mu\nu}(K) \gamma^\mu S^{(0)}(Q) \gamma^\nu, \quad (5.30)$$

as illustrated in Fig. 5.4. Here, $Q = P - K$ and the integration is carried out only for soft momenta.

The considerations of Appendix A to evaluate the frequency sum and then find

the imaginary part of Eq.(5.30) after analytic continuation are simplified by the presence of the bare quark propagator. In the long wavelength limit $|\vec{p}| \rightarrow 0$ the mass-shell condition $p_0 = m$ imposed on $\delta(p_0 + k_0 - \omega(q))$ implies that $q_0 \simeq m$ and $k_0 \simeq \vec{k}^2/2m$. The other δ -functions that arise have no support in this region of interest. As will be seen in the next Section, Ward identities can be used to show that the gauge dependent contributions to Eq.(5.30) are proportional to the mass-shell condition, and apart from some concerns to be discussed shortly that arise in certain gauges [66], such terms will not contribute to this order. One then finds the discontinuity of the self-energy of Eq.(5.30) in this limit is given by the gauge independent result

$$\begin{aligned} \text{Im}_p^* \Sigma(p) &= -\frac{m_g^2 TC_f}{2\pi} \int_0^\infty dk \left[2(\gamma^0 - 1) \mathfrak{S}_k \frac{1}{k_t^2} + (\gamma^0 + 1) \mathfrak{S}_k \frac{1}{\mathbf{k}_t^2} \right] \\ &= -(\gamma^0 - 1) \frac{3g^2 TC_f m_g^2}{16\pi \mu_{cutoff}^2} - (\gamma^0 + 1) \frac{g^2 TC_f}{16\pi}. \end{aligned} \quad (5.31)$$

The first term with the infrared cutoff contributes to wave function renormalization, while the second term shifts the pole. Eq.(5.29) can be modified to the present situation by inserting a mass term and neglecting the hard thermal contribution $\delta\Sigma$; hence, up to the leading order of both real ($\sim gT$) and imaginary ($\sim g^2T$) parts, in the long wavelength limit,

$$S^{-1}(p_0, \vec{p} = 0) = p_0 \gamma^0 - m - i(\gamma^0 + 1)a \quad (5.32)$$

where $a = g^2 TC_f / (16\pi)$ and only the relevant term has been kept. The solution $\omega = m - ig^2 TC_f / 8\pi$ to the dispersion relation thus has an imaginary part, which leads to a damping rate [64].

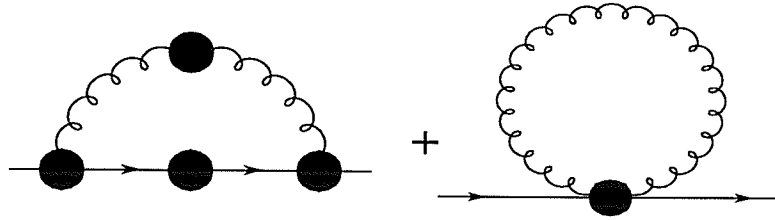


Figure 5.5: Resummed fermion propagator

5.2.2 Massless quark

For a massless quark in the long wavelength limit, the one-loop approximation to the fermion self-energy generally leads to a gauge dependent damping constant, as happens for pure gluons [10]. The use of the effective propagators and vertices in the calculation will be seen to formally give a gauge independent answer, but is significantly more involved in the massless case than in the heavy fermion case because all the effective propagators and vertices must be included [63, 64, 29].

The quark self-energy

The resummed quark self-energy

$$*\Sigma(P) = \Sigma_{(1)}(P) + \Sigma_{(2)}(P) \quad (5.33)$$

as illustrated in Fig. 5.5 consists of two distinct terms [64, 29]: one from the quark-gluon loop,

$$\Sigma_{(1)}(P) = g^2 C_f \int_{soft} dK * \Gamma^\mu(P, Q) * S(q) * \Gamma^\nu(Q, P) D_{\mu\nu}(K), \quad (5.34)$$

where $Q = P - K$, and the other from the single gluon loop,

$$\Sigma_{(2)}(P) = \frac{1}{2}g^2C_f \int_{soft} dK D_{\mu\nu}(K) {}^*\Gamma^{\mu\nu}(P, P; K, K). \quad (5.35)$$

We first examine the gauge dependent terms. The term linearly proportional to the gauge parameter $\lambda(K)$ of Eq.(5.33) is given by

$$\begin{aligned} & -g^2C_f \int \frac{dK}{k_l^2} \lambda(K) (\tilde{n}_\mu K_\nu + \tilde{n}_\nu K_\mu) \times \\ & \quad \left[{}^*\Gamma^\mu(P, Q) {}^*S(Q) {}^*\Gamma^\nu(Q, P) + \frac{1}{2} {}^*\Gamma^{\mu\nu}(P, P; K, K) \right] \\ & = -g^2C_f \int \frac{dK}{k_l^2} \lambda(K) \tilde{n}_\mu \times \\ & \quad \left[{}^*\Gamma^\mu(P, Q) {}^*S(Q) {}^*S^{-1}(P) + {}^*S^{-1}(P) {}^*S(Q) {}^*\Gamma^\mu(Q, P) \right], \end{aligned} \quad (5.36)$$

where the Ward identities of Eqs.(5.21) and (5.28) have been used. The remaining gauge dependent terms, again using Eqs.(5.21) and (5.28), can be written as

$$\begin{aligned} & g^2C_f \int dK \left[\frac{c^2(K)}{K^4} - \frac{\lambda^2(K)}{k_l^2} \right] K_\mu K_\nu \times \\ & \quad \left[{}^*\Gamma^\mu(P, Q) {}^*S(Q) {}^*\Gamma^\nu(Q, P) + \frac{1}{2} {}^*\Gamma^{\mu\nu}(P, P; K, K) \right] \\ & = g^2C_f \int dK \left[\frac{c^2(K)}{K^4} - \frac{\lambda^2(K)}{k_l^2} \right] \left[{}^*S^{-1}(P) {}^*S(Q) {}^*S^{-1}(P) - {}^*S^{-1}(P) \right], \end{aligned} \quad (5.37)$$

Thus, both gauge dependent terms of Eqs.(5.36) and (5.37) are proportional to ${}^*S^{-1}(P)$, and will vanish when the mass-shell condition is imposed if the associated integrals are not singular in this limit. Recently these integrals have been examined in detail, and questions were raised concerning the neglect of such terms in certain gauges, particularly the usual covariant gauges, in both the fermion and gluon damping rate calculations to lowest order [66]. This problem was subsequently shown to

be related to the introduction of an infrared cutoff and the resulting question of when such a cutoff should be taken to zero as the mass-shell limit is approached [67]. We will postpone our discussion of this point until chapter 6.

We thus drop the gauge dependent terms of Eqs.(5.36) and (5.37) on mass-shell, and consider only the gauge independent contributions to Eq.(5.33). Two such terms arise. One, from the transverse gluons, is found in the long wavelength limit to be

$$\begin{aligned}
& g^2 C_f \int \frac{dK}{k_t^2} A_{\mu\nu} \left[{}^* \Gamma^\mu(P, Q) {}^* S(Q) {}^* \Gamma^\nu(Q, P) + \frac{1}{2} {}^* \Gamma^{\mu\nu}(P, P; K, K) \right] \\
&= -g^2 C_f \gamma_0 \int \frac{dK}{k_t^2} \left\{ 2\chi_0(q_0, k) \left[1 - \frac{m_f^2 q_0}{2k^2 p_0} - \frac{1}{2p_0} \left(1 - \frac{q_0^2}{k^2} \right) \xi_0(q_0, k) \right]^2 \right. \\
&\quad \left. + \frac{1}{p_0^2} \left[1 - \frac{q_0^2}{k^2} \right] \xi_0(q_0, k) \right\}, \tag{5.38}
\end{aligned}$$

where only terms relevant to the imaginary part are retained. The other gauge independent contribution, from the plasmon mode, is in the long wavelength limit

$$\begin{aligned}
& -g^2 C_f \int \frac{dK}{k_t^2} \tilde{n}_\mu \tilde{n}_\nu \left[{}^* \Gamma^\mu(P, Q) {}^* S(Q) {}^* \Gamma^\nu(Q, P) + \frac{1}{2} {}^* \Gamma^{\mu\nu}(P, P; K, K) \right] \\
&= -g^2 C_f \gamma_0 \int \frac{dK}{k_t^2} \left\{ \left[\frac{k^2}{p_0^2} + \left(2 - \frac{k_0}{p_0} \right)^2 \right] \chi_0(q_0, k) \right. \\
&\quad \left. - \frac{2k}{p_0} \left(2 - \frac{k_0}{p_0} \right) \chi_s(q_0, k) \right\}. \tag{5.39}
\end{aligned}$$

The total contribution to the imaginary part of the quark self-energy then becomes

$$\begin{aligned}
& -\gamma_0 g^2 C_f \text{Im}_p \int dK \left\{ \frac{1}{k_t^2} \left[\frac{1}{4p_0^2 k^2} \left[(2p_0 - k_0 + k)^2 (k_0 + k)^2 \Delta_+(q_0, k) \right. \right. \right. \\
&\quad \left. \left. + (2p_0 - k_0 - k)^2 (k_0 - k)^2 \Delta_-(q_0, k) \right] + \frac{1}{2p_0^2} \left(1 - \frac{q_0^2}{k^2} \right) \xi_0(q_0, k) \right] \\
&\quad \left. + \frac{1}{2p_0^2 k_t^2} \left[(2p_0 - k_0 - k)^2 \Delta_+(q_0, k) + (2p_0 - k_0 + k)^2 \Delta_-(q_0, k) \right] \right\}. \tag{5.40}
\end{aligned}$$

The damping constant

The frequency sum and the extraction of the imaginary part after analytic continuation of Eq.(5.40) can be performed using the considerations of Appendix. In this case, in addition to the contributions from the poles, there are terms arising from the cuts. On mass-shell in the high temperature, long wavelength limit, we find for Eq.(5.40)

$$\begin{aligned}
\text{Im}_p^* \Sigma(p_0 = m_f, p = 0) = & -\gamma_0 \frac{g^2 T C_f}{2\pi} \int_0^\infty k^2 dk \int_0^\infty \frac{dk_0}{k_0} \times \\
& \left\{ \frac{(k - k_0 + 2m_f)^2 (k + k_0)^2}{4m_f^2 k^2} \mathfrak{S}_k \frac{1}{k_t^2} \mathfrak{S}_p \Delta_+(q_0, k) \right. \\
& + \frac{(k + k_0 - 2m_f)^2 (k - k_0)^2}{4m_f^2 k^2} \mathfrak{S}_k \frac{1}{k_t^2} \mathfrak{S}_p \Delta_-(q_0, k) \\
& + \frac{(k + k_0 - 2m_f)^2}{2m_f^2} \mathfrak{S}_k \frac{1}{k_t^2} \mathfrak{S}_p \Delta_+(q_0, k) \\
& + \frac{(k - k_0 + 2m_f)^2}{2m_f^2} \mathfrak{S}_k \frac{1}{k_t^2} \mathfrak{S}_p \Delta_-(q_0, k) \\
& \left. + \frac{1}{4k^3} (k^2 - q_0^2) \mathfrak{S}_k \frac{1}{k_t^2} \theta(k^2 - q_0^2) \right\}. \tag{5.41}
\end{aligned}$$

One can verify that the same result of Eq.(5.41) is obtained using the dispersion relation methods of Refs.[64, 32]. Since in Eq.(5.41) $\mathfrak{S}_k[1/k_t^2]/k_0$, $\mathfrak{S}_k[1/k_t^2]/k_0$, $\mathfrak{S}_p \Delta_+$ and $\mathfrak{S}_p \Delta_-$ are all positive definite, $\text{Im}_p \Sigma(p_0 = m_f, p = 0)$ is negative definite, which will leads to a positive definite damping constant which we are going to derive. Since, in the long wavelength limit, $D_0(p_0, \mathbf{p} = 0) = (p_0 - m_f^2/P_0)\gamma_0$, the dispersion relation determined by (5.29) becomes

$$p_0 - \frac{m_f^2}{p_0} - i \frac{1}{4} \text{Tr}[\gamma_0 \text{Im}_p^* \Sigma] = 0 \tag{5.42}$$

which leads to the solution

$$p_0 = m_f + i\frac{1}{8}\text{Tr}[\gamma_0^*\Sigma(\mathbf{p} = 0)]. \quad (5.43)$$

It is convenient in Eq.(5.41) to rescale $k_0 \rightarrow m_f k_0$ and $k \rightarrow m_f k$. If a tilde symbol above a function denotes its form after such a rescaling, i.e., $\tilde{f}(\omega, k) \equiv \frac{1}{m_f^D} f(m_f \omega, m_f k)$ if the function $f(\omega, k)$ has dimension D , then with the damping constant defined as

$$\gamma(p = 0) = -\frac{1}{8}\text{Tr} [\gamma_0 \text{Im}_p^* \Sigma(p_0 = m_f, p = 0)] \equiv a(N, N_f) \frac{g^2 T C_f}{4\pi}, \quad (5.44)$$

one obtains

$$a(N, N_f) = a_{pole-pole} + a_{pole-cut} + a_{cut-cut} \quad (5.45)$$

where

$$\begin{aligned} & a_{pole-pole} \\ = & \frac{[k + \tilde{\omega}_t(k)]^2 [k - \tilde{\omega}_t(k) + 2]^2 \tilde{R}_t(\tilde{\omega}_t(k), k) \tilde{R}(\tilde{\omega}_+(k), k)}{4\tilde{\omega}_t(k) |\tilde{\omega}'_t(k) - \tilde{\omega}'_+(k)|} \Bigg|_{\tilde{\omega}_t(k) - \tilde{\omega}_+(k) = 1} \\ & - \frac{[k - \tilde{\omega}_t(k)]^2 [k + \tilde{\omega}_t(k) - 2]^2 \tilde{R}_t(\tilde{\omega}_t(k), k) \tilde{R}(\tilde{\omega}_-(k), k)}{4\tilde{\omega}_t(k) |\tilde{\omega}'_t(k) - \tilde{\omega}'_-(k)|} \Bigg|_{\tilde{\omega}_t(k) - \tilde{\omega}_-(k) = 1} \\ & + \frac{k^2 [k - \tilde{\omega}_l(k) + 2]^2 \tilde{R}_l(\tilde{\omega}_l(k), k) \tilde{R}(\tilde{\omega}_+(k), k)}{2\tilde{\omega}_l(k) |\tilde{\omega}'_l(k) - \tilde{\omega}'_+(k)|} \Bigg|_{\tilde{\omega}_l(k) - \tilde{\omega}_+(k) = 1} \\ & + \frac{k^2 [k + \tilde{\omega}_l(k) - 2]^2 \tilde{R}_l(\tilde{\omega}_l(k), k) \tilde{R}(\tilde{\omega}_-(k), k)}{2\tilde{\omega}_l(k) |\tilde{\omega}'_l(k) - \tilde{\omega}'_-(k)|} \Bigg|_{\tilde{\omega}_l(k) - \tilde{\omega}_-(k) = 1}, \quad (5.46) \end{aligned}$$

$$\begin{aligned} & a_{pole-cut} \\ = & -\frac{1}{4} \int \frac{dk}{\tilde{\omega}_t(k)} \tilde{R}_t(\tilde{\omega}_t(k), k) \theta[k - |\tilde{\omega}_t(k) - 1|] \times \end{aligned}$$

$$\begin{aligned}
& \left\{ [k + \tilde{\omega}_t(k)]^2 [k - \tilde{\omega}_t(k) + 2]^2 \tilde{\beta}_+(1 - \tilde{\omega}_t(k), k) \right. \\
& \quad \left. + [k - \tilde{\omega}_t(k)]^2 [k + \tilde{\omega}_t(k) - 2]^2 \tilde{\beta}_-(1 - \tilde{\omega}_t(k), k) - \frac{1}{k} (k^2 - (1 - \tilde{\omega}_t(k))^2) \right\} \\
& + \frac{1}{2} \int \frac{k^2 dk}{\tilde{\omega}_l(k)} \tilde{R}_l(\tilde{\omega}_l(k), k) \theta[k - |\tilde{\omega}_l(k) - 1|] \times \\
& \quad \left\{ [k + \tilde{\omega}_l(k) - 2]^2 \tilde{\beta}_+(1 - \tilde{\omega}_l(k) + [k - \tilde{\omega}_l(k) + 2]^2 \tilde{\beta}_-(1 - \tilde{\omega}_l(k), k)) \right\} \\
& - \frac{1}{4} \int_0^\infty \frac{dk}{1 - \tilde{\omega}_+(k)} \tilde{R}(\tilde{\omega}_+(k), k) \times \\
& \quad \left\{ [k + \tilde{\omega}_+(k) + 1]^2 [k - \tilde{\omega}_+(k) + 1]^2 \tilde{\beta}_t(1 - \tilde{\omega}_+(k), k) \right. \\
& \quad \left. - 2k^2 [k - \tilde{\omega}_+(k) - 1]^2 \tilde{\beta}_l(1 - \tilde{\omega}_+(k), k) \right\} \\
& - \frac{1}{4} \int_0^\infty \frac{dk}{1 - \tilde{\omega}_-(k)} \tilde{R}(\tilde{\omega}_-(k), k) \times \\
& \quad \left\{ [k - \tilde{\omega}_-(k) - 1]^2 [k + \tilde{\omega}_-(k) - 1]^2 \tilde{\beta}_t(1 - \tilde{\omega}_-(k), k) \right. \\
& \quad \left. - 2k^2 [k + \tilde{\omega}_-(k) + 1]^2 \tilde{\beta}_l(1 - \tilde{\omega}_-(k), k) \right\}, \tag{5.47}
\end{aligned}$$

$$\begin{aligned}
& a_{cut-cut} \\
= & -\frac{1}{4} \int_{\frac{1}{2}}^\infty dk \int_{1-k}^k \frac{dk_0}{k_0} \left\{ \tilde{\beta}_t(k_0, k) \left[[k + k_0]^2 [k - k_0 + 2]^2 \tilde{\beta}_+(1 - k_0, k) \right. \right. \\
& \quad \left. \left. + [k - k_0]^2 [k + k_0 - 2]^2 \tilde{\beta}_-(1 - k_0, k) - \frac{1}{k} (k^2 - (1 - k_0)^2) \right] \right. \\
& \quad \left. - 2k^2 \tilde{\beta}_l(k_0, k) \left[(k + k_0 - 2)^2 \tilde{\beta}_+(1 - k_0, k) + (k - k_0 + 2)^2 \tilde{\beta}_-(1 - k_0, k) \right] \right\}. \tag{5.48}
\end{aligned}$$

The terms in Eq.(5.46) are pole-pole contributions, the terms in Eq.(5.47) are pole-cut terms, and Eq.(5.48) is the cut-cut term. The above expressions were evaluated numerically and the results are listed in Table 5.1. For $SU(3)$ with $N_f = 2$ no pole-pole terms contribute and $a(N, N_f) = 1.399$. For $SU(2)$ with $N_f = 2$, one

	$N=3, N_f = 2$	$N=2, N_f = 2$	$N=2, N_f = 4$
pole-pole	0.00	0.010	0.080
pole-cut	0.900	0.885	0.873
cut-cut	0.500	0.556	0.620
$a(N, N_f)$	1.40	1.45	1.57

Table 5.1: Results for the damping rate for 3 different combinations of N and N_f .

pole-pole term from the transverse gluon and negative fermion mode contributes and $a(N, N_f) = 1.451$. For $SU(2)$ with $N_f = 4$, all four pole-pole terms contribute and $a(N, N_f) = 1.573$.

5.3 Summary

We have examined the calculation of the lowest order damping rate of heavy and massless fermions in hot gauge theories in the long wavelength limit using the resummation techniques developed recently in terms of hard thermal loops. An approach was used to evaluate the Matsubara frequency sum and extract the imaginary part of the resulting analytically continued expressions which gave the same final results as those found by dispersion relation methods [64, 32]. Apart from questions raised recently concerning the neglect in some gauges of certain terms proportional to the mass-shell condition [66, 67], gauge independent results for this rate were obtained in a wide class of gauges. Ward identities between the effective propagators and vertices simplified significantly the calculations, and the answers obtained, both in magnitude and in sign, indicate that these techniques give tractable and reasonable

results.

Chapter 6

Gauge Dependence Revisited

In the previous chapter Ward identities have been used to show the gauge fixing independence of the damping rate by showing that the relevant gauge dependent part of the resummed loop diagrams is proportional to the inverse fermion propagator, and hence formally vanishes in the mass shell limit. However, the gauge independence of the damping rate was subsequently questioned by the calculations of the on-shell limit of the gluon resummed loop diagram performed in covariant gauge in [66], where the infrared divergent double pole integral that is multiplied by a small parameter, $\zeta^2 \sim (\omega^2 - \omega_{pole}^2)^2$, has been effectively cut from below by ζ , which leaves in the damping a finite gauge dependent piece with the same lowest order, $g^2 T$, as the gauge independent part. A resolution to this problem was subsequently proposed by Rebhan [67] (see also [68, 70]), who showed that if an infrared regulator was introduced in the loop integral and then removed *after* the mass-shell limit, $\zeta \rightarrow 0$, is imposed, the gauge dependent contribution vanishes. The situation became more transparent when this on-shell limit problem was shown to be univer-

sal and is totally unrelated to the resummation method but also occurred in the bare one-loop diagrams [71].

One the other hand, related to the thermal Drell-Yan mechanism in the ultra-relativistic heavy ion collisions, the infrared and mass singularities of the radiative corrections to the production rate of lepton pairs in QGP has also been studied intensively [71, 72]. In this chapter, we are going to link the necessity of keeping an infrared cutoff in the gauge dependence problem with the cancellation of infrared divergences in the two loop virtual photon polarization tensor in a heat bath [35].

We first briefly review the gauge dependence problem for the fermion damping constant. As the problem is not confined to the Braaten–Pisarski resummation scheme, we consider the simpler case of the bare one-loop fermion self-energy. For this, the gauge dependent term contributing to the imaginary part is

$$\Sigma_{G.D.}(p) \sim S^{-1}(p) \left[\frac{1}{\alpha} g^2 C_f \int \frac{d^4 k}{(2\pi)^4} \frac{1}{k^4} S(p-k) \right] S^{-1}(p) \equiv S^{-1}(p) I(p) S^{-1}(p), \quad (6.1)$$

where $S^{-1}(p) = \not{p} - m$ and α is the covariant gauge parameter. Following the prescriptions employed by the authors of Ref.[66], the on-shell limit of the imaginary part of the above integral that is sandwiched between the inverse propagators can be evaluated by expanding in terms of $\zeta = (P^2 - m^2)$ and one obtains

$$\text{Im } I(p) \sim -\frac{p_0}{4\pi\alpha} g^2 T (\not{p} + m) \frac{1}{\zeta^2} \quad (6.2)$$

which, as stated above, has been effectively cut off at ζ due to the lack of an obvious intrinsic infrared regulator of the theory. The existence of a genuine cutoff, either physically motivated [73] or required by consistency of perturbation theory, will in general change the on-shell behaviour of the self-energy. For instance, if an infrared regulator is introduced in $I(p)$ of Eq.(6.1), the expansion of $I(p)$ around

the mass-shell is no longer singular at $p^2 = m^2$ for finite values of the regulator [67]. Taking the mass-shell limit $p^2 \rightarrow m^2$ first and then removing the infrared regulator thus leads to a vanishing contribution to $\text{Tr} [(p' + m)\text{Im}\Sigma_{G.D.}(p)]$, and hence to a gauge independent result for the damping rate. However, a non-vanishing result will be obtained if no such regulator is used due to the cancellation of ζ between the numerator and denominator.

Although an infrared regulator is in general needed, for example, to define the zero temperature wave-function counterterm, its introduction in this specific infrared finite one-loop term may appear unusual. Such a “regularization” of finite integrals does occur, however, at higher orders. For instance, if in the limit as some regulating parameter ϵ is removed one has an infinite and a finite integral, the expansion of the product of the two integrals,

$$\int dk F(k) \int dl G(l) \sim \left[\frac{A}{\epsilon} + B + \dots \right] [C + D\epsilon + \dots], \quad (6.3)$$

has the correct finite part only if the term proportional to ϵ is included. We will be particularly interested in the case where the singular parts of two such terms cancel, as in the example

$$\begin{aligned} \frac{a}{b} - 1 &= \int_0^\infty dx \left[1 - \frac{x}{\sqrt{x^2 + a^2}} \right] \int_0^\infty \frac{y dy}{(y^2 + b^2)^{3/2}} - \int_0^1 dx \int_1^\infty \frac{dy}{y^2} \\ &= \lim_{\Lambda \rightarrow \infty} \left\{ \int_0^\Lambda dx \left[1 - \frac{x}{\sqrt{x^2 + a^2}} \right] \int_0^\Lambda \frac{y dy}{(y^2 + b^2)^{3/2}} \right. \\ &\quad \left. - \int_0^1 \frac{x dx}{\sqrt{x^2 + a^2/\Lambda^2}} \int_1^\infty \frac{y dy}{(y^2 + b^2/\Lambda^2)^{3/2}} \right\} \\ &= \lim_{\Lambda \rightarrow \infty} \left\{ \int_0^\Lambda dx \int_0^\Lambda \frac{y dy}{(y^2 + b^2)^{3/2}} - \frac{1}{b} \int_0^\Lambda \frac{x dx}{\sqrt{x^2 + a^2}} \right\}. \end{aligned} \quad (6.4)$$

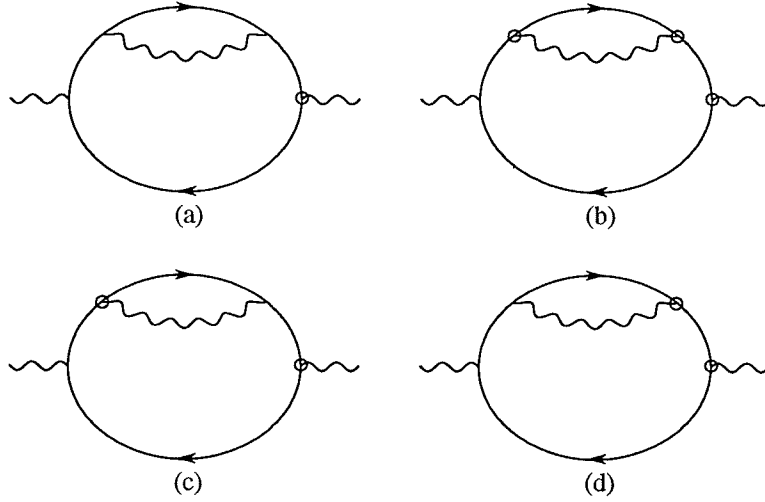


Figure 6.1: Two loop photon polarization tensor with the self-energy correction

Note that the last y integral is finite by itself as $\Lambda \rightarrow \infty$, but since

$$\lim_{\Lambda \rightarrow \infty} \left\{ \int_0^\Lambda dx \int_0^\infty \frac{y dy}{(y^2 + b^2)^{3/2}} - \frac{1}{b} \int_0^\Lambda \frac{x dx}{\sqrt{x^2 + a^2}} \right\} = \frac{a}{b} \neq \frac{a}{b} - 1, \quad (6.5)$$

the limit $\Lambda \rightarrow \infty$ in Eq.(6.4) must be taken after the integrals have been evaluated.

We consider now an analogous example involving the one-loop fermion self-energy

$$\Sigma(p) \sim \int dk D_{\mu\nu}(k) \gamma^\mu S(p-k) \gamma^\nu, \quad (6.6)$$

and focus in particular on the contribution of the imaginary part, which is relevant to the one-loop damping rate. This example is provided by the decay rate of a photon calculated from the imaginary part of the two-loop photon self-energy. We use real time Cutkosky rules to calculate this rate [74, 75], with the relevant “cuts” of the photon self-energy shown in Fig.6.1. The “virtual” contributions involving the insertion of the one-loop self-energy $\Sigma(p)$ of Eq.(6.6) are shown in Figs.6.1(a,b,c),

which at zero temperature are normally taken into account by placing a wave-function counterterm on the fermion line. With

$$\begin{aligned} n_F(p) &= \frac{1}{e^{\beta|p_0|} + 1}, \\ \Delta_p &= \frac{i}{p^2 - m^2 + i\epsilon}, \\ S^\pm(p) &= (\not{p} + m) [\theta(\pm p_0) - n_F(p)] 2\pi\delta(p^2 - m^2), \end{aligned} \quad (6.7)$$

these terms can be written as

$$-g^2 \int \frac{d^4p}{(2\pi)^4} [\theta(p_0) - n_F(p)] \text{Tr} \left[\gamma_\mu S^-(p - q) \gamma_\nu (\not{p} + m) F_p (\not{p} + m) \right], \quad (6.8)$$

where

$$F_p = \text{Im} \Sigma_{11}(p) (\Delta_p + \Delta_p^*)^2 \epsilon(p_0) \coth(\beta p_0) - i \text{Re} \Sigma_{11}(p) (\Delta_p - \Delta_p^*)^2 \quad (6.9)$$

and

$$\begin{aligned} \text{Re} \Sigma(p) &= \text{Re} \Sigma_{11}(p), \\ \text{Im} \Sigma(p) &= \epsilon(p_0) \coth(\beta p_0/2) \text{Im} \Sigma_{11}(p) \end{aligned} \quad (6.10)$$

relates the Feynman self-energy $\Sigma(p) \equiv \Sigma(i\omega_n \rightarrow p_0 + i\epsilon p_0)$ to the function $\Sigma_{11}(p)$ arising in real time finite temperature Feynman rules [74, 75]. We then add the “real” contribution of Fig.6.1(d) corresponding to photon emission and/or absorption; this has the same form as Eq. (6.8) with the replacement of F_p by

$$\text{Im} \Sigma_{11}(p) \epsilon(p_0) \left[(\Delta_p \Delta_p + \Delta_p^* \Delta_p^*) \coth(\beta p_0/2) - (\Delta_p + \Delta_p^*)^2 \coth(\beta p_0) \right]. \quad (6.11)$$

As is the case at zero temperature, the addition of this “real” term to the “virtual” term of Eq.(6.8) causes the pinch singularities $\Delta_p \Delta_p^*$ to cancel, leaving the result

$$\begin{aligned} &-g^2 \int \frac{d^4p}{(2\pi)^4} [\theta(p_0) - n_F(p)] \times \\ &\quad \times \text{Tr} \left\{ \gamma_\mu S^-(p - q) \gamma_\nu (\not{p} + m) 2 \text{Re} [\Delta_p (-i\Sigma(p)) \Delta_p] (\not{p} + m) \right\}. \end{aligned} \quad (6.12)$$

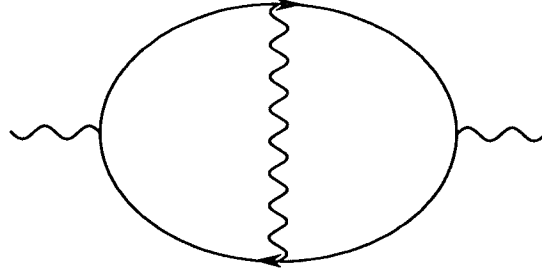


Figure 6.2: Two loop photon polarization tensor with the vertex correction

Eq.(6.12) represents our example of a two-loop integral involving the one-loop $\Sigma(p)$ of Eq.(6.6). Note that, because

$$\text{Re} [\Delta_p(-i\Sigma(p))\Delta_p] = \pi \text{Re} \Sigma(p) \frac{\partial \delta(p^2 - m^2)}{\partial m^2} + \text{Im} \Sigma(p) \text{Re} \left[\frac{1}{(p^2 - m^2 + i\epsilon)^2} \right], \quad (6.13)$$

Eq.(6.12) is sensitive in particular to the behaviour of $\text{Im} \Sigma(p)$ near the mass-shell $p^2 = m^2$. Now, as shown in Refs.[71, 72], both terms in Eq.(6.12) involving $\text{Re} \Sigma(p)$ and $\text{Im} \Sigma(p)$ are separately infrared divergent. These divergences eventually cancel; in the Feynman gauge this occurs amongst topologically similar diagrams as in Fig.6.1, but in general gauge invariance may demand the inclusion of the imaginary part of the graph of Fig.6.2 with the vertex correction for such a cancellation. In any case, the presence of such divergences on a term-by-term basis forces one to introduce an infrared regulator in evaluating the integrals and isolating the singularities.

There are two features here that bear resemblance to the resolution of the gauge dependence problem of the one-loop damping rate [67, 68, 71, 70]. One is that in

the two-loop integral of Eq.(6.12) an infrared regulator is introduced in the term containing the imaginary part of the one-loop $\Sigma(p)$ of Eq.(6.6). As discussed after Eq.(6.4), such a regulator is needed even though it is not required for the one-loop term alone, and it is removed only after the integrals have been performed and the infrared singularity isolated for eventual cancellation against other sources. The other feature is that, as seen from Eq.(6.13), Eq.(6.12) is sensitive to the behaviour of $\text{Im}\Sigma(p)$ near the mass-shell $p^2 = m^2$. In effect, then, in this calculation $\text{Im}\Sigma(p)$ is probed around the mass-shell in the presence of a finite infrared regulator. This qualitatively is similar to the procedure of Refs.[67, 68, 71, 70] used to resolve the gauge dependence problem of the one-loop damping rate: evaluate $\text{Im}\Sigma(p)$ on-shell in the presence of a finite infrared regulator. These considerations indicate that this procedure, which perhaps appears unusual at the one-loop level, does arise in the context of a higher-order calculation in a natural way.

Chapter 7

Conclusions

In this thesis we have been interested in the study through finite temperature field theories of the properties of hot QCD plasma. Linear response analysis has been carried out to extract physical poles from the gluon propagator through the Dyson's equation in which the gluon polarization tensor $\Pi_{\mu\nu}$ which in a number of gauges is not transverse perturbatively, i.e. $k^\mu \Pi_{\mu\nu} \neq 0$. The resulting equations determining the response of the transverse and of the longitudinal modes, which different from the normally used expressions for the transverse self-energy, are expressed in terms of the (transverse and longitudinal) coefficients of the self-energy. We have examined high temperature QCD at the one-loop level in both covariant gauges and regulated static temporal gauge in which the polarization tensor is not transverse, hence the non-transverse coefficient $\Phi \neq 0$ in general. One finds to this order of approximation in both gauges the equations for the longitudinal and for the transverse modes coincide separately in the long wavelength limit. Both gauges give the same plasma frequency, $\omega_p^2 = g^2 NT^2/9$. While covariant gauges give a gauge fixing dependent damping

constant of the order of g^2T , the damping rate in the regulated static temporal gauge is independent of the gauge parameter $0 < \alpha < 1$. In the static limit, both gauges give essentially the same behaviours for the longitudinal and for the transverse modes in infrared region. One obtains gauge fixing independent expression for the longitudinal pole with chromo-electric mass squared $m_{el}^2 = g^2NT^2/3$, and the well known Landau ghost problem for the transverse mode.

The above mentioned problems in the one-loop calculations show the necessity of searching for a gauge invariant and self-consistent expansion scheme rather than the usual loop expansion. In particular, one of such scheme proposed by Braaten and Pisarski, which incorporates all relevant higher loop diagrams in terms of the “hard thermal loops”, has been used to calculate the fermion damping rate to order g^2T in the long wavelength limit. The excitation spectra of the gluon and massless fermion have been obtained and illustrated in Fig. 5.1 and Fig. 5.2 respectively. Ward identities between the effective propagator and vertices have been derived and subsequently been used to formally prove the gauge independence of the damping rate to this order. The damping rate then obtained is gauge independent and positive definite which indicates that these techniques give tractable and reasonable results.

However, recent studies show that an infrared cutoff plays a crucial role in obtaining gauge independent damping rates for hot gauge theories calculated within this scheme. The gauge dependent contribution to the lowest order damping rate, which being proportional to the inverse propagator, formally vanishes on-shell only if an infrared regulator was introduced in the loop integral and then removed *after* the mass-shell limit is imposed. We have argued in the light of the cancellation of the infrared divergences that occurred in the two-loop photon polarization tensor that

such procedure for the resolution of the gauge dependent problem, which perhaps appears unusual at the one-loop level, does arise in the context of a higher-order calculation in a natural way.

Other problems deserving further study are the Landau ghost problem which appears in the previous one-loop calculations and the related problem of the existence of chromo-magnetic mass. It is generally believed that the resolutions to these problems require non-perturbative analyses. Some interesting results along this line have already been obtained [76] which suggests the vanishing of magnetic mass within a small but infinite subset of (ladder) diagrams. In this regard the generalization of the eikonal picture of gauge theories [77] to finite temperature may be useful to investigate the infrared behaviour of the hot QCD.

Finally, perhaps it is worth mentioning that the Braaten and Pisarski resummation method does not solve the fast fermion damping problem. A self-consistent scheme is needed to evaluate the damping rate through the Schwinger-Dyson equation [24, 69]. However, this procedure only works for real mass-shell condition but not for complex one [73] and the reason for that is still an unsolved problem.

Appendix A

Frequency sums

In this appendix we give some technical details of the evaluation of the Matsubara frequency sums and of the calculation of the imaginary part of the subsequent analytically continued expressions [37]. Consider a frequency sum at finite temperature in the imaginary time formalism involving a bosonic function $f(k_0 = i2\pi nT)$ - the extension of the following to include fermions is straightforward. Evaluate the frequency sum by [37]

$$T \sum_{n=-\infty}^{+\infty} f(k_0 = i2\pi nT) = \frac{1}{4\pi i} \oint_{\mathcal{C}} dk_0 \coth \left[\frac{k_0}{2T} \right] f(k_0), \quad (\text{A.1})$$

where the continuation $i2\pi nT \rightarrow k_0 + i\epsilon$ to real energies is made and the integration contour \mathcal{C} encircles the poles of the hyperbolic function counter-clockwise.

Suppose now the complex function $f(k_0)$ decays sufficient rapidly at infinity. The

sum can be rewritten as the following:

$$\sum_{n=-\infty}^{n=+\infty} f(z = i2\pi nT) = - \{ \text{sum of residues of } \pi f(z) \cot(\pi z) \text{ at all the poles of } f(z) \}. \quad (\text{A.2})$$

Here we list the results of the frequency sums evaluated from (A.2) that will be needed in the analysis of the polarization tensor of chapter 4. In the following, $p_0 = 2\pi inT$.

$$T \sum_n \frac{N(p_0)}{p^2} = -\frac{1}{4E_1} \coth\left(\frac{E_1}{2T}\right) [N(E_1) + N(-E_1)] \quad (\text{A.3})$$

$$T \sum_n \frac{N(p_0)}{p_0^2 + a^2 \vec{p}^2} = \frac{1}{4aE_1} \cot\left(\frac{aE_1}{2T}\right) [N(iaE_1) + N(-iaE_1)] \quad (\text{A.4})$$

$$T \sum_n \frac{N(p_0)}{p^2 q^2} = -\frac{1}{4E_1} \coth\left(\frac{E_1}{2T}\right) \left[\frac{N(E_1)}{(k_0 + E_1)^2 - E_2^2} + (E_1 \rightarrow -E_1) \right] \\ - \frac{1}{4E_2} \coth\left(\frac{E_2}{2T}\right) \left[\frac{N(-E_2 - k_0)}{(k_0 + E_2)^2 - E_1^2} + (E_2 \rightarrow -E_2) \right] \quad (\text{A.5})$$

$$T \sum_n \frac{N(p_0)}{(p_0^2 + a^2 \vec{p}^2)(q_0^2 + a^2 \vec{q}^2)} \\ = \frac{1}{4aE_1} \cot\left(\frac{aE_1}{2T}\right) \left[\frac{N(iaE_1)}{(k_0 + iaE_1)^2 + a^2 E_2^2} + (E_1 \rightarrow -E_1) \right] \\ + \frac{1}{4aE_2} \cot\left(\frac{aE_2}{2T}\right) \left[\frac{N(-iaE_2 - k_0)}{(k_0 + iaE_2)^2 + a^2 E_1^2} + (E_2 \rightarrow -E_2) \right] \quad (\text{A.6})$$

$$\begin{aligned}
T \sum_n \frac{N(p_0)}{p^2(q_0^2 + a^2 \vec{q}^2)} &= -\frac{1}{4E_1} \coth\left(\frac{E_1}{2T}\right) \left[\frac{N(E_1)}{(k_0 + E_1)^2 + a^2 E_2^2} + (E_1 \rightarrow -E_1) \right] \\
&+ \frac{1}{4aE_2} \cot\left(\frac{aE_2}{2T}\right) \left[\frac{N(-iaE_2 - k_0)}{(k_0 + iaE_2)^2 - E_1^2} + (E_2 \rightarrow -E_2) \right]
\end{aligned} \tag{A.7}$$

$$\begin{aligned}
T \sum_n \frac{N(p_0)}{p^2(p_0^2 + a^2 \vec{p}^2)(q_0^2 + a^2 \vec{q}^2)} &= \\
&-\frac{(1-\alpha)}{4E_1^3} \coth\left(\frac{E_1}{2T}\right) \left[\frac{N(E_1)}{(k_0 + E_1)^2 + a^2 E_2^2} + (E_1 \rightarrow -E_1) \right] \\
&-\frac{(1-\alpha)}{4aE_1^3} \cot\left(\frac{aE_1}{2T}\right) \left[\frac{N(iaE_1)}{(k_0 + iaE_1)^2 + a^2 E_2^2} + (E_1 \rightarrow -E_1) \right] \\
&+ \frac{1}{4aE_2} \cot\left(\frac{aE_2}{2T}\right) \left[\frac{N(-iaE_2 - k_0)}{[(k_0 + iaE_2)^2 - E_1^2][(k_0 + iaE_2)^2 + a^2 E_1^2]} + (E_2 \rightarrow -E_2) \right]
\end{aligned} \tag{A.8}$$

$$\begin{aligned}
T \sum_n \frac{N(p_0)}{p^2 q^2 (p_0^2 + a^2 \vec{p}^2)(q_0^2 + a^2 \vec{q}^2)} &= \\
&-\frac{(1-\alpha)}{4E_1^3} \coth\left(\frac{E_1}{2T}\right) \left[\frac{N(E_1)}{[(k_0 + E_1)^2 - E_2^2][(k_0 + E_1)^2 + a^2 E_2^2]} + (E_1 \rightarrow -E_1) \right] \\
&-\frac{(1-\alpha)}{4E_2^3} \coth\left(\frac{E_2}{2T}\right) \left[\frac{N(-E_2 - k_0)}{[(k_0 + E_2)^2 - E_1^2][(k_0 + E_2)^2 + a^2 E_1^2]} + (E_2 \rightarrow -E_2) \right] \\
&-\frac{(1-\alpha)}{4aE_1^3} \cot\left(\frac{aE_1}{2T}\right) \left[\frac{N(iaE_1)}{[(k_0 + iaE_1)^2 - E_2^2][(k_0 + iaE_1)^2 + a^2 E_2^2]} + (E_1 \rightarrow -E_1) \right] \\
&-\frac{(1-\alpha)}{4aE_2^3} \cot\left(\frac{aE_2}{2T}\right) \left[\frac{N(-iaE_2 - k_0)}{[(k_0 + iaE_2)^2 - E_1^2][(k_0 + iaE_2)^2 + a^2 E_1^2]} + (E_2 \rightarrow -E_2) \right]
\end{aligned} \tag{A.9}$$

where $E_1 = |\vec{p}|$ and $E_2 = |\vec{q}| = |\vec{p} + \vec{k}|$. Recall that we have assumed that $0 < \alpha < 1$

so that a is real in these expressions.

For a function $f(k_0)$ with not only has poles but also discontinuities, the above analysis, in particular Eq.(A.2), would not be sufficient. Let us consider first a complex function $f(x)$ defined on the real axis. The inverse of this function will have an imaginary part related to its discontinuity across the real axis as

$$\Im_x \frac{1}{f(x)} \equiv -\frac{1}{\pi} \text{Im}_x \frac{1}{f(x)} = \frac{1}{2\pi i} \left[\frac{1}{f(x-i\epsilon)} - \frac{1}{f(x+i\epsilon)} \right]. \quad (\text{A.10})$$

Contributions to this imaginary part come from zeroes of the function, giving rise to residue terms, and from cut terms due to discontinuities of f across the real axis. A residue contribution to $\Im_x(1/f(x))$ for $1/f(x)$ with a simple pole at $x = x_0$ will have the form

$$\frac{1}{f'(x_0)} \delta(x - x_0) \equiv R_f(x_0) \delta(x - x_0). \quad (\text{A.11})$$

For a cut term, suppose $f(x)$ has a cut for $0 < x < a$, and define in this interval $f(x+i\epsilon) = f^R(x) + if^I(x)$ and $f(x-i\epsilon) = f^R(x) - if^I(x)$. The contribution of this cut to Eq.(A.10) will have the form

$$\frac{1}{\pi} \frac{f^I(x)}{f^R(x) + f^{I2}(x)} \theta(x) \theta(a-x) \equiv \beta_f(x) \theta(x) \theta(a-x). \quad (\text{A.12})$$

Including both the pole and cut terms, Eq.(A.10) then becomes

$$\Im_x \frac{1}{f(x)} = R_f(x_0) \delta(x - x_0) + \beta_f(x) \theta(x) \theta(a-x). \quad (\text{A.13})$$

This formula can readily be generalized to cases with multiple poles and cuts.

Consider now a frequency sum as in (A.1). The contour can be deformed and split into two pieces : one encircling the real axis and the other forming a great circle at infinity. Since $1/(e^{|k_0|/T} - 1)$ damps at large $|k_0|$, only poles and cuts of f

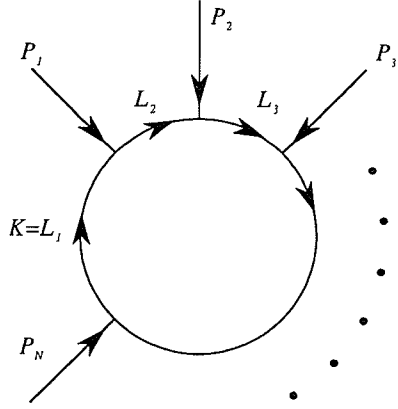


Figure A.1: One loop amplitude

which appear along the real axis will contribute. We then have, using Eq.(A.13),

$$T \sum_{n=-\infty}^{+\infty} f(k_0 = i2\pi nT) = -\frac{1}{2} \int_{-\infty}^{+\infty} dk_0 \coth \left[\frac{k_0}{2T} \right] \Im_k f(k_0). \quad (\text{A.14})$$

Extending the above considerations to a one loop diagram with N incoming momenta, P_i , $i = 1, \dots, N$ as shown in Fig. A.1. The notation $P = (p_0, \vec{p})$ will be used to denote the 4-momentum. The loop momenta L_i for $i = 1, \dots, N$ will be given by $L_1 \equiv K$ and $L_i = K + \sum_{j=1}^{i-1} P_j$ for $i > 1$. The scattering amplitude of Fig. A.1 will in general have the following form

$$A(P_i) = T \sum \int \frac{d^3k}{(2\pi)^3} V(L_1, \dots, L_N) \prod_{i=1}^N f_i(L_i) \quad (\text{A.15})$$

where $V(L_1, \dots, L_N)$ comes from the vertices and hence is analytic everywhere along the real axis. The function f_i depends only on L_i and has singularities along the

real axis of the L_i -plane. Analogous to (A.14), one finds

$$A(P's) = -\frac{1}{2} \int \frac{d^3 k}{(2\pi)^3} \int_{-\infty}^{+\infty} dk_0 V(L's) \sum_{j=1}^N \left(S_j \Im_{L_{j_0}} f_j \prod_{i \neq j} f_i \right) \quad (\text{A.16})$$

where $S_i = \coth \left[\frac{L_{i_0}}{2T} \right]$ if L_i is bosonic and $S_i = \tanh \left[\frac{L_{i_0}}{2T} \right]$ if L_i is fermionic.

We apply the above considerations to a fermion self-energy correction:

$$\begin{aligned} & \Sigma(p_0 = i(2n+1)\pi T, \vec{p}) \\ &= T \sum_m \int \frac{d^3 k}{(2\pi)^3} f(K) g(P-K) \\ &\equiv \int dK f(k_0 = i2\pi mT, \vec{k}) g(q_0 = i(2(n-m)+1)\pi T, \mathbf{q}) \\ &= -\frac{1}{2} \int \frac{d^3 k}{(2\pi)^3} \int_{-\infty}^{+\infty} dk_0 (S_K \Im f(K) g(Q) + S_Q \Im g(Q) f(K)) \quad (\text{A.17}) \end{aligned}$$

and $Q = P - K$. The extension of Eq.(A.14) to include functions which involve an external energy $p_0 = i2\pi nT$ is straightforward, and after such an evaluation of the frequency sum the analytic continuation $i2\pi nT \rightarrow p_0 + i\epsilon$ is made. This continuation results in the function acquiring an imaginary part, which can subsequently be extracted by use of Eqs.(A.10) and (A.13). Such a procedure, with modifications as necessary, are used in the calculations of chapter 5, and can be seen to lead to the same final answer as that found by the spectral representation methods of Refs.[64, 32].

Bibliography

- [1] E. Witten, Phys. Rev. **D30**, 272 (1984);
D.N. Schramm, Nucl. Phys. **B252**, 53 (1985).
- [2] E.V. Shuryak, Phys. Rep. **61**, 71 (1980).
- [3] J.C. Collins and M.I. Perry, Phys. Rev. Lett. **34**, 1353 (1975).
- [4] J.I. Kapusta, Nucl. Phys. **B 148**, 461 (1979).
- [5] E.V. Shuryak, Phys. Rep. **61**, 71 (1980).
- [6] A.M. Polyakov, Phys. Lett. **B 72**, 477 (1978).
- [7] L. Susskind, Phys. Rev. **D 20**, 2610 (1979).
- [8] O.K. Kalashnikov and V.V. Klimov, Phys. Lett. **B 88**, 328 (1980).
- [9] V. V. Klimov, Sov. J. Nucl. Phys. **33**, 934 (1981);
Sov. Phys. JETP **55**, 199 (1982).
- [10] See "Status of perturbative thermal QCD", Physica **A158** (1989).
- [11] K. Kajantie and J. Kapusta, Ann. Phys. **160**, 477 (1985).

- [12] U. Heinz, K. Kajantie, and T. Toimela, Phys. Lett. **B 183**, 96 (1987).
- [13] U. Heinz, K. Kajantie, and T. Toimela, Ann. Phys. **176**, 218 (1987).
- [14] T.H. Hansson and I. Zahed, Phys. Rev. Lett. **58**, 2397 (1987).
- [15] T.H. Hansson and I. Zahed, Nucl. Phys. **B 292**, 725 (1987).
- [16] H.-Th. Elze, U. Heinz, K. Kajantie, and T. Toimela, Z. Phys. **C 37**, 305 (1988).
- [17] A. Linde, Rep. Progr. Phys. **42**, 389 (1979); Phys. Lett. **B 96**, 289 (1980).
- [18] O.K. Kalashnikov and V.V. Klimov, Sov. J. Nucl. Phys. **33**, 443 (1981).
- [19] H.-Th. Elze, K. Kajantie, and T. Toimela, Z. Phys. **C 37**, 601 (1988).
- [20] S. Nadkarni, Phys. Rev. Lett. **61**, 396 (1988).
- [21] S. Nadkarni, "The nonperturbative quark-gluon plasma", University of Kentucky report UK/88-05, April, 1988.
- [22] R. Pisarski, "Scattering amplitudes in hot gauge theories", Fermilab preprint 88/123-T, Sept., 1988.
- [23] R. Pisarski, "How to compute scattering amplitudes in hot gauge theories", Fermilab preprint 88/113-T, Nov., 1988.
- [24] V.V. Lebedev and A.V. Smilga, Ann. Phys. **202**, 229 (1990).
- [25] S. Coleman and E. Weinberg, Phys. Rev. **D 7**, 1888 (1973).
- [26] J.S. Kang, Phys. Rev. **D 10**, 3455 (1974).

- [27] R. Kobes, G. Kunstatter and A. Rebhan, Phys. Rev. Lett. **64**, 2992 (1990); Nucl. Phys. **B355**, 1 (1991).
- [28] H. A. Weldon, Phys. Rev. **D26**, 1384, 2789 (1982).
- [29] E. Braaten and R. D. Pisarski, Nucl. Phys. **B337**, 569 (1990); **B339**, 310 (1990); Brookhaven Report BNL-46 (unpublished).
- [30] J. C. Taylor and S. M. H. Wong, Nucl. Phys. **B346**, 115 (1990).
- [31] J. Frenkel and J. C. Taylor, Nucl. Phys. **B334**, 199 (1990); Z. Phys. **C49**, 515 (1991); DAMTP Report (unpublished).
- [32] E. Braaten and R. D. Pisarski, Phys. Rev. Lett. **64**, 1338 (1990); Phys. Rev. **D42**, 2156 (1990).
- [33] R. Kobes, G. Kunstatter and K. Mak, Phys. Lett. **B223**, 433 (1989); Z. Phys. **C45**, 129 (1989).
- [34] R. Kobes, G. Kunstatter and K. Mak, Phys. Rev. **D45**, 4632 (1992).
- [35] R. Kobes and K. Mak, Phys. Rev. **D** (to be published).
- [36] A.L. Fetter and J.D. Walecka, *Quantum Theory of Many-Particle Systems*, McGraw-Hill (1971).
- [37] N. P. Landsman and Ch. G. Van Weert, Phys. Rep. **145**, 141 (1987).
- [38] J.I. Kapusta, *Finit-Temperature Field Theory*, (Cambridge University Press, 1989).
- [39] F.J. Dyson, Phys. Rev. **75**, 486 (1949); 1736 (1949).

- [40] R.P. Feynman and A.R. Hibbs, *Quantum Mechanics and Path Integrals*, (McGraw-Hill, New York, 1965).
- [41] F.A. Berezin, *Theor. Math. Phys.* **6**, 141 (1971);
R.F. Dashen, B. Hasslacher and A. Neveu, *Phys. Rev.* **D 12**, 2443 (1975);
Y. Ohnuki and T. Kashiwa, *Prog. Theor. Phys.* **60**, 548 (1978).
- [42] L. Faddeev and V. Popov, *Phys. Lett.* **25B**, 29 (1967).
- [43] C. Bernard, *Phys. Rev.* **D 9**, 3312 (1974);
H. Hata and T. Kugo, *Phys. Rev.* **D 21**, 3333 (1980).
- [44] T. Matsubara, *Prog. Theor. Phys.* **14**, 351 (1955).
- [45] H. Matsumoto, Y. Nakano, H. Umezawa, F. Mancini and M. Marinaro, *Progr. Theor. Phys.* **70**, 599 (1983);
H. Matsumoto, Y. Nakano and H. Umezawa, *J. Math. Phys.* **25**, 3076 (1984).
- [46] H. Matsumoto, I. Ojima and H. Umezawa, *Ann. Phys.* **152**, 348 (1984).
- [47] P.C. Martin and J. Schwinger, *Phys. Rev.* **115**, 1342 (1959).
- [48] A. Burnel, *Phys. Rev.* **D36**, 1852 (1987).
- [49] C. Itzykson and J.-B. Zuber, *Quantum Field Theory*, (McGraw-Hill, New York, 1980).
- [50] G. Kunstatter, *Can. J. Phys.* (to be published).
- [51] R. Kobes and G. Kunstatter, *Phys. Rev. Lett.* **61**, 392 (1988).
- [52] A. Rebhan, *Nucl. Phys.* **B 288**, 832 (1987).

- [53] W. Kummer, *Acta Phys. Austriaca* **41**, 315 (1975).
- [54] M.E. Carrington, H. Yamagishi, and I. Zahed, "The timelike axial gauge at zero and finite temperature", Stony Brook preprint, 1988.
- [55] M.E. Carrington, T.H. Hansson, H. Yamagishi, and I. Zahed, "Linear response of hot gluons", Stony Brook preprint, 1988.
- [56] S. Nadkarni, *Phys. Rev. D* **27**, 917 (1983).
- [57] J. Frenkel and J.C. Taylor, *Nucl. Phys. B* **109**, 439 (1976).
- [58] A. Burnel, *Phys. Rev. D* **36**, 1852 (1987).
- [59] O.K. Kalashnikov, V.V. Klimov and E. Casado, *Phys. Lett. B* **114**, 49 (1982).
- [60] J.M. Cornwall, *Phys. Rev. D* **26**, 1453 (1982).
- [61] J.M. Cornwall and W.-S. Hou, *Phys. Lett. B* **153**, 173 (1985).
- [62] O.K. Kalashnikov and V.V. Klimov, *Sov. J. Nucl. Phys.* **31**, 699 (1980);
D.J. Gross, R.D. Pisarski and L.G. Yaffe, *Rev. Mod. Phys.* **53**, 43 (1981).
- [63] R. D. Pisarski, *Physica A***158**, 146, 246 (1989).
- [64] R. D. Pisarski, *Phys. Rev. Lett.* **63**, 1129 (1989);
*Nucl. Phys. A***498**, 423c (1989).
- [65] H. A. Weldon, *Physica A***158**, 169 (1989); *Phys. Rev. D***40**, 2410 (1989).
- [66] R. Baier, G. Kunstatter, and D. Schiff, *Phys. Rev. D***45**, 4381 (1992); *Nucl. Phys. B***388**, 287 (1992).

- [67] A. Rebhan, Phys. Rev. **D46**, 4779 (1992).
- [68] E. Braaten and R. Pisarski, Phys. Rev. **D46**, 1829 (1992).
- [69] T. Altherr, E. Petitgirard, T. del Rio Gaztelurrutia, Phys. Rev. **D47**, 703 (1993).
- [70] H. Nakkagawa, A. Niegawa and B. Pire, Phys. Lett. **B294**, 396 (1992).
- [71] T. Altherr, P. Aurenche and T. Becherrawy, Nucl. Phys. **B315**, 436 (1989).
- [72] T. Altherr and T. Becherrawy, Nucl. Phys. **B330**, 174 (1990).
- [73] A. V. Smilga, BUTP-92/39.
- [74] R. L. Kobes and G. W. Semenoff, Nucl. Phys. **B260**, 714 (1985); Nucl. Phys. **B272**, 329 (1986).
- [75] N. Ashida, H. Nakkagawa, H. Yokota and A. Niegawa, Ann. Phys. **215**, 315 (1992).
- [76] A.P. de Almeida and J. Frenkel, Phys. Rev. **D47**, 640 (1993).
- [77] J.M. Cornwall and G. Tiktopoulos, Phys. Rev. **D15**, 2937 (1977).